Final Report Submitted to the Office of Naval Research

July, 1993

Title : Experimental Investigation of Turbulent Prandtl Number and Reynolds Analogy in Transitional and Post-Transitional Boundary Layers

Grant No. : N00014-89-J-3105

Principle Investigator :

Ting Wang, Associate Professor
Department of Mechanical Engineering
Clemson University

ONR Program Monitor :

Dr. Gabriel Roy

Final Report Submitted to the Office of Naval Research

July, 1993

Title : Experimental Investigation of Turbulent Prandtl Number and Reynolds Analogy in Transitional and Post-Transitional Boundary Layers

Grant No. : N00014-89-J-3105

Principle Investigator :

Ting Wang, Associate Professor
Department of Mechanical Engineering
Clemson University

ONR Program Monitor :

Dr. Gabriel Roy

Statement A per telecon
Dr. Gabriel Roy ONR/Code 1132
Arlington, Va 22217-5000

NWW 10/4/93

ABSTRACT

The effects of elevated free-stream turbulence and streamwise acceleration on flow and thermal structures in transitional boundary layers have been investigated experimentally on a heated flat plate. The effects on the turbulent Prandtl number and Reynolds analogy were included in this study. The free-stream turbulence levels ranged from 0.5 to 7%, and the acceleration strengths, based on K ($\equiv(\nu/\bar{u}_\infty^2)d\bar{u}_\infty/dx$), ranged from 0.39×10^{-6} to 4.1×10^{-6}. A three-wire probe was used to measure the detailed momentum and thermal boundary layer structures, including the streamwise and cross-stream velocity fluctuations, the temperature fluctuation, the Reynolds stresses, the Reynolds heat fluxes, the eddy viscosity, the turbulent thermal diffusivity and the turbulent Prandtl number. The results show that elevated free-stream turbulence values result in an earlier onset of transition and reduced length of transition, whereas streamwise acceleration delays the onset of transition and lengthens the transition region, even at elevated FSTI. Compared to streamwise acceleration, FSTI is the more dominant factor on flow and thermal structure in transitional boundary layers; however, streamwise acceleration significantly reduces the turbulent spot formation rate. A conditional sampling technique was utilized to separate the flow into the turbulent and nonturbulent portions. An analysis of flow and thermal structures was performed in each portion separately.

TABLE OF CONTENTS

EXECUTIVE SUMMARY

Introduction and Statement of Work

A multi-year project to investigate the flow and thermal structures in the transitional boundary layer was performed during a period from 1989 to 1993. A detailed description of the program and its results are written as a final technical report submitted to the Office of Naval Research (see publication on page 9). Only a summary is provided in this final report.

Transitional boundary layer theory is heavily dependent upon the results of experimental studies. Most reported experimental studies of the effects of elevated free-stream turbulence intensity (FSTI) and its combined effects with streamwise acceleration on boundary layer transition investigated only the onset and end of transition. The results of the few experimental investigations which detailed boundary layer measurements were made with elevated free-stream turbulence effects and its combined effects with streamwise acceleration are insufficient to represent the flow and thermal boundary layer characteristics resulting from these effects.

The main objective of this study is to investigate experimentally the effects of elevated free-stream turbulence and its combined effects with streamwise acceleration on the flow and thermal structures, including on the turbulent Prandtl number and the Reynolds analogy in the transitional boundary layers with the following specific goals:

(1) to document and investigate these effects on the onset and end of transition, the mean and RMS velocity and temperature profiles, the Reynolds shear stress, the Reynolds heat fluxes and the turbulent Prandtl number in the transitional boundary layer flows,

(2) to investigate the incoherence between the momentum and the thermal transport in the transition region under the separate and combined effects of elevated free-stream turbulence and favorable pressure gradients, and

(3) to use a conditional sampling technique to obtain the intermittency distributions and to investigate the flow and thermal behavior in the separated nonturbulent and turbulent portions of a transitional boundary layer.

In order to investigate the effects of elevated free-stream turbulence and streamwise acceleration on the flow and thermal structures in the transitional boundary layers, two kinds of measurements were performed : (1) the heat transfer and skin friction on the wall and (2) the detailed boundary layer measurements using a miniature 3-wire probe. The elevated FSTI required for this study are generated by three turbulence generating grids with different mesh widths. The streamwise acceleration parameter, K, is kept constant in the test section by setting the test section into a wedge shape. For the streamwise accelerating case, the wall heat transfer measurements of sixteen cases were made first. Then four accelerating cases were chosen for detailed boundary layer measurements. The highest K value is 4.1×10^{-6}. In total, eight cases with detailed measurements were investigated at different FSTI and streamwise pressure gradients K :

Baseline Case : No Grid, FSTI = 0.5%, K = 0 (shared with Keller, 1993)
G1K0 Case : Grid 1, FSTI = 3.3%, K = 0
G2K0 Case : Grid 2, FSTI = 5.6%, K = 0
G3K0 Case : Grid 3, FSTI = 6.4%, K = 0
G1K1 Case : Grid 1, FSTI = 3.8%, $K = 0.39 \times 10^{-6}$
G1K2 Case : Grid 1, FSTI = 3.8%, $K = 0.83 \times 10^{-6}$
G3K2 Case : Grid 3, FSTI = 6.4%, $K = 0.83 \times 10^{-6}$
G3K3 Case : Grid 3, FSTI = 6.4%, $K = 1.00 \times 10^{-6}$.

For each case, the following physical entities are collected and reduced : (a) the momentum transport (Mean velocity profiles, Reynolds normal and shear stresses, intermittency across the boundary layer and along the streamwise direction, integral and dissipation length scales, turbulence and thermal power spectra, eddy diffusivity and skin-friction coefficient) and (b) the thermal transport (Mean and rms temperature profiles, Reynolds heat fluxes, turbulent thermal diffusivity, Stanton number and turbulent Prandtl number).

Experimental Facility and Equipment

Wind Tunnel

The present research employed a 2-D, open-circuit, blowing-type wind tunnel. The detailed description of the design considerations and the construction specifications were documented by Kuan (1987) and Kuan & Wang (1990). Air is drawn through a filter box, then forced through two grids, a honeycomb, a heat exchanger, a screen pack and a contraction nozzle before entering the test section (Fig. 1). The flow rate can be adjusted steplessly from 0.5 m/s to 35 m/s by the combined use of an inlet damper and a constant-torque, variable frequency motor controller. The steadiness of the free-stream velocity and temperature can be maintained within 1% and 0.5^{o}C for a 24-hour period, and the uniformity is within 0.7% and 0.1^{o}C, respectively.

Test Section

The rectangular test section is 0.15m wide, 2.4m long and 0.92m high with an aspect ratio of 6. The large aspect ratio reduces edge effects and ensures the two dimensionality of the boundary layer flow. One of the test section walls served as the test wall (Fig. 2). The heat patch inside the test wall was constructed of a serpentine heater foil sandwiched between glass cloth and silicon rubber sheets. A 1.56 mm thick aluminum sheet was vulcanized to the front surface of the heater pad to ensure uniformity of the heat flux. A 1.56 mm polycarbonate sheet was placed on the aluminum surface to provide a smooth test surface on which the air flows and measurements were taken. The surface temperature was measured by 184 3mil E-type thermocouples which were embedded strategically inside the test wall to capture the streamwise and spanwise variation of wall heat transfer in a transitional boundary layer (Fig. 3). Fourteen measuring holes were drilled along the outer observation wall centerline in the test section and measurements were obtained by traversing the probe through these holes into the test section. Boundary layer suction was applied at the leading edge of the test section so that a near zero thickness boundary layer can be achieved at the leading edge. The detailed construction consideration

and description of the heated test wall are contained in Wang et al. (1992) and Zhou (1993).

Turbulence Generating Grids

The background FSTI of this wind tunnel was about 0.5 percent. The higher turbulence levels required for this study were generated by inserting various turbulence generating grids into the wind tunnel. The turbulence generating grids consisted of bi-plane rectangular bar arrays with approximately a 69% open area (Fig. 4). The grids were designed based on the recommendation of Baines and Peterson (1951) to produce test section turbulence levels ranging from approximately 3 to 7%. Grid generated turbulence decays with distance from the grid. The decaying rate becomes smaller when the distance from the grid increases. In order to generate homogeneous and slowly decaying turbulence, the turbulence generating grids were inserted at the entrance to the main tunnel contraction instead of placing them at the inlet of the test section. The grids are referred to as grid 1, 2, and 3, corresponding to the mesh widths, M, of 19.05, 24.13 and 33.02 cm, respectively. The test case with only background turbulence (no grid) served as the baseline case.

Flow Acceleration

In this experiment, the streamwise acceleration parameter, K, is kept constant in the test section simply by setting the test section into a wedge shape. It should be noted that a constant K flow is inherently different from a Falkner-Skan flow, which has a constant Λ ($\equiv(\delta^2/\nu)d\bar{U}_\infty/dx$) value (see discussion by Zhou and Wang, 1992).

Three-Wire Probe

A three-wire sensor was specifically designed to measure simultaneously the instantaneous longitudinal velocity, cross-stream velocity and the temperature. The development and qualification of this three-wire sensor was described by Shome (1991) and Wang et al. (1992).

Basically, an 'X' array, consisting of gold plated tungsten wires 1.0 mm long and 2.5 μm in diameter, is used for measuring velocity. The sensing length is 0.5 mm and is etched in the center (Fig. 5). The spacing between the 'X' array is 0.35 mm. The temperature sensor is a 0.35 mm long (with a sensing length of 0.35 mm) and a 1.2 μm diameter unplated platinum wire placed in a plane parallel to the plane of the crossed wires and spaced 0.35 mm from the 'X' array. To allow for near-wall measurement and to reduce probe interference, the probe support was bent at an angle of 10° from the wire axis. However, the x-wires are still perpendicular to each other.

To sufficiently extend the length of transition for detailed measurements on the test wall, extremely low-speed flows down to 1.7 m/s are provided for elevated FSTI cases. At this low speed, relatively low overheat ratios for the x-wires are required to minimize the "cross-talk" between the x-wires and the temperature sensor (Zhou and Wang, 1993). The X-wires are operated at an overheat ratio of about 1.2 (hot wires) in the constant temperature mode. The 1.2 μm platinum wire is operated at a very low current of 0.1 mA (cold wire) in the constant current mode.

Summary of Results

Summary of Elevated Free-stream Turbulence Effects

Low free-stream velocities (~ 2 m/s) were used to obtain a sufficient laminar-turbulent transition region. Wall heat transfer measurements indicated that elevated FSTI values result in an earlier onset of transition and reduced length of transition in terms of Re_x, $Re\delta^*$, and $Re\theta$ (Fig. 6, Table 1). The calculated turbulent spot formation rates at elevated FSTI cases agree with Mayle's correlation (Fig. 7). In the turbulent region, the mean velocity and temperature profiles demonstrate the logarithmic "law of the wall" characteristics over a sufficient range of Y^+ (30~300) (Figs. 8 & 9). The wake regions are completely depressed.

The u' distribution is significantly elevated across the entire boundary layer in the laminar and turbulent regions due to elevated FSTI (Fig. 10). In the transitional region, the maximum Reynolds normal

stresses, which reflect the bursting activities in the boundary layer, are higher than the baseline case but are limited to approximately $u'/\overline{U}_\infty$=20%. The $u'/\overline{U}_\infty$ distribution in the turbulent region is found to be affected by the low Reynolds number (Fig. 11). The peak value of $u'/\overline{U}_\infty$ is higher for lower Reynolds number. The evolution of the rms temperature fluctuation is similar to the u' with elevated values across 80% of the boundary layer (Fig. 12).

The v' distribution in the outer boundary layer is controlled by the magnitude of v' in the free stream (Fig. 13). The typical near-wall peak of v', which appears in the transition region at low FSTI, is not observed. In the turbulent region, the very near-wall peak of v' is suppressed and the largest v' value occurs away from the wall in elevated FSTI cases. This implies that elevated FSTI does not affect near-wall v' as it does to u'.

The evolution of the $\overline{uv}$ distribution at elevated FSTI is similar to that at low FSTI (Fig. 14). In the transition region, Reynolds shear stress is produced not in the near-wall region where the vigorous turbulence production of u' occurs but away from the wall, at about y/δ=0.3. This high turbulent shear progresses toward the wall and eventually affects the wall shear.

The $-\overline{ut}/\{q''_w/\rho C_p\}$ distributions are elevated in the laminar and turbulent regions but are reduced in the transitional region at higher FSTI (Fig. 15). Since both u' and t' are higher in the elevated FSTI case than the baseline case, this indicates that the correlation between u and t at low FSTI is much better than that at elevated FSTI in transitional boundary layer flow.

The $\overline{vt}$ distributions reach maximum values in the transition region slower than the evolution of $\overline{ut}$ (Fig. 16). The regions of negative values of $\overline{vt}$ occur in the transition region in the baseline case and are not observed in the elevated FSTI cases.

In the near wall region (y/δ<0.2), the turbulent Prandtl number values are large (>2) (Fig. 17). In the region of y/δ=0.2 ~ 0.8, the turbulent Prandtl number values are close to 1.2 ~ 1.6. These higher turbulent Prandtl numbers in the transitional and low-Reynolds-number turbulent flow should be considered in the numerical modeling of transitional boundary layers.

Summary of Combined Effects of Elevated Free-Stream Turbulence and Streamwise Acceleration

Wall heat transfer measurements indicated that elevated FSTI values result in an earlier onset of transition and reduced length of transition, whereas the streamwise accelerations delay the onset of transition and lengthen the transition region even at elevated FSTI (Figs. 18, 19 & 20, Table 2). A mild acceleration has a significant effect on onset and end of transition, whereas further increasing acceleration does not significantly augment its effect on onset of transition (Fig. 21).

At elevated FSTI, the streamwise acceleration has a negligible effect on $\overline{T}$, u', v', t',$\overline{vt}$, and Pr_t distributions and has a mild effect on $\overline{ut}$ distributions across the boundary layers (Figs. 22, 23, 24, 25, 26, 27 & 28). A noticeable effect of acceleration on the flow structure can be seen in both $\overline{U}$ and the $\overline{uv}$ distributions (Figs. 29 & 30). Overall, in the range of FSTI tested by this study(3~7%), the effect of FSTI is more pronounced than that of the acceleration on the onset of transition; however, the effect of acceleration on the length of transition cannot be ignored, especially at a higher FSTI, at which the end of transition Re_x is about ten times of the onset of transition Re_x for $K>0.83x10^{-6}$ (Figs. 18 & 19).

Summary of Conditional Sampling Results

The streamwise evolution of the intermittency factor profiles across the boundary layer are processed for the present experimental cases. The detailed conditional sampling results for the baseline case were documented by Keller (1993). The $(duv/d\tau)^2$ is chosen as the criterion function. The method for determining the threshold value and the intermittency factor is explained by Zhou (1993). Similar to the conditional sampling results of the baseline case, (a) the threshold values of $(duv/d\tau)^2$ have a nearly constant value regardless of the streamwise and cross-stream location (Fig. 31); (b) the intermittency varies across the boundary layer and has a maximum value away from the wall in the boundary layer for all elevated FSTI and accelerating cases (Figs. 32a,b,c,d,e,f,g); (c) the skin friction in

the nonturbulent and turbulent portions do not behave as a simple extension of laminar and turbulent flow respectively (Fig. 33).

The conditionally sampled statistical results for all the mean and turbulent structures are presented. At elevated FSTI, the magnitudes of u', t' and $\overline{ut}$ in the turbulent part are about the same as those in the non-turbulent part (Figs. 34, 35 & 36). However, the magnitudes of v' in the turbulent part are much higher than those in the nonturbulent part (Fig. 37).

OTHER PERSONNEL ASSOCIATED WITH THIS PROGRAM

1. Dadong Zhou, a doctoral student supported by this ONR grant, is expected to graduate in August 1993.

2. F. Jeffery Keller, a doctoral student mainly supported by an AFOSR grant, was supported by this ONR grant for three months. He graduated in June 1993.

3. Biswadip Shome, a master student supported by a graduate assistantship from Clemson University, developed the three-wire probe to measure the Reynolds stresses and heat fluxes for this program. He finished his master's degree program at Clemson in August 1991.

PUBLICATIONS

Refereed Journal Publications

"Effects of Elevated Free-Stream Turbulence on Flow and Thermal Structures in Transitional Boundary Layers," Zhou, D., and Wang, T., accepted for publication in the ASME *Journal of Turbomachinery*.

"Effects of Different Criterion Functions on Intermittency in Heated Transitional Boundary Layers with and without Streamwise Accelerations." Keller, F.J., and Wang, T., accepted for publication in the ASME *Journal of Turbomachinery*.

Refereed Conference Papers

"Combined Effects of Elevated Free-Stream Turbulence and Streamwise Acceleration on Flow and Thermal Structures in Transitional Boundary Layers," Zhou, D., and Wang, T., to be presented at the 1993 National Heat Transfer Conference at Atlanta, Georgia.

"Effects of Elevated Free-Stream Turbulence on Flow and Thermal Structures in Transitional Boundary Layers," Zhou, D., and Wang, T., presented at the 1993 ASME International Gas Turbine and Aeroengine Congress and Exposition, Cincinnati, Ohio. ASME paper 93-GT-66.

"Effects of Different Criterion Functions on Intermittency in Heated Transitional Boundary Layers with and without Streamwise Accelerations," Keller, F.J., and Wang, T., presented at the 1993 ASME International Gas Turbine and Aeroengine Congress and Exposition, Cincinnati, Ohio. ASME paper 93-GT-67.

"Experimental Investigation of Reynolds Shear Stresses and Heat Fluxes in a Transitional Boundary Layer," Wang, T., Keller, F.J., and Zhou, D., ASME HTD-Vol. 226, Fundamental and Applied Heat Transfer Research for Gas Turbine Engine, pp. 61-70, 1992.

"Laminar Boundary Layer Flow and Heat Transfer with Favorable Pressure Gradient at Constant K Values," Zhou, D., and Wang T., presented at the 1992 ASME International Gas Turbine and Aeroengine Congress and Exposition. ASME paper 92-GT-246.

Technical Reports

"Development of Three-Wire Probe for the Measurement of Reynolds Stresses and Heat Fluxes in the Transitional Boundary Layer," Wang, T., and Shome, B., August, 1991.

"Effects of Elevated Free-stream Turbulence and Streamwise Acceleration on Flow and Thermal Structures in Transitional Boundary Layers," Zhou, D., and Wang, T., Final Technical Report submitted to ONR, 1993.

NOMENCLATURE

C_f = skin friction coefficient, $t_w/(\rho\bar{U}_\infty^2/2)$

FSTI = free-stream turbulence intensity, $\sqrt{(u^2+v^2+w^2)/3}/\bar{U}_\infty$

K = streamwise acceleration parameter, $(\nu/\bar{U}_\infty^2)d\bar{U}_\infty/dx$

n = turbulent spot production rate (no./(m·s))

$\hat{n}$ = dimensionless turbulent spot production rate, $n\nu^2/\bar{U}_\infty^3$

Pr_t = turbulent Prandtl number, $\varepsilon_M/\varepsilon_H$

q" = heat flux

Re_x,Re_{δ^*},Re_θ= Reynolds numbers based on x, δ^* & θ

St = Stanton number, $q''_w/[\rho c_p\bar{U}_\infty(\bar{T}w-\bar{T}_\infty)]$

t = instantaneous temperature fluctuation or time

t' = rms value of t

$\bar{T}$ = mean temperature

T^+ = mean temperature in wall units, $(\bar{T}_w-\bar{T})\rho c_p u^*/q''_w$

u, v = instantaneous streamwise & cross-stream velocity fluctuations

u', v' = rms values of u & v

$u^* \equiv \sqrt{\tau_w/\rho}$,friction velocity

$\bar{U}$ = mean streamwise velocity

U^+ = mean streamwise velocity in wall units

x = streamwise distance from leading edge

x_o = unheated starting length

y = distance away from the wall

$Y^+ = yu^*/\nu$

α = thermal diffusivity

δ = boundary layer thickness at $0.995\bar{U}_\infty$

δ^* = displacement boundary layer thickness

θ = momentum boundary layer thickness

Γ = intermittency

$\Lambda \equiv (\delta^2/\nu)d\bar{U}_\infty/dx$

ν = kinematic viscosity

ρ = density

σ = turbulent spot propagation parameter

τ = shear stress

Subscripts

e = at the end of the transition

s = at the start of the transition

w = at the wall

∞ = in the free-stream

REFERENCES

Baines, W.D. and Peterson, E.G., 1951, "An Investigation of Flow Through Screens," *Trans. ASME*, Vol. 73, pp. 467-480.

Blair, M.F., 1982, "Influence of Free-Stream Turbulence on Boundary Layer Transition in Favorable Pressure Gradients," ASME *Journal of Engineering for Power*, Vol. 104, pp. 743-750.

Blair, M.F., 1983a, "Influence of Free-Stream Turbulence on Turbulent Boundary Layer Heat Transfer and Mean Profile Development, Part I - Experimental Data," *ASME J. Heat Transfer*, Vol. 105, pp. 33-40.

Blair, M.F., 1983b, "Influence of Free-Stream Turbulence on Turbulent Boundary Layer Heat Transfer and Mean Profile Development, Part II - Analysis of Results," *ASME J. Heat Transfer*, Vol. 105, pp. 41-47.

Chua, L.P. and Antonia, R.A., 1990, "Turbulent Prandtl Number in a Circular Jet," *International Journal of of Heat and Mass Transfer*, Vol. 33, No. 2, pp. 331-339.

Dyban, Y.P., Epik, E.Y., and Suprun, T.T., 1980, "Characteristics of the Laminar Boundary Layer in the Presence of Elevated Free-Stream Turbulence," *Fluid Mech.-Soviet Research* (in English), Vol. 22, No. 5, pp. 213-228.

Graham, R.W., 1979, "Fundamental Mechanisms that Influence the Estimate of Heat Transfer to Gas Turbine Blades," ASME paper 79-HT-43.

Graham, R.W. (editor), 1984, *Transition in Turbines*, NASA TM-79128.

Hinze, J.O., 1975, *Turbulence*, 2nd ed., McGraw-Hill, New York.

Keller, F.J., 1993, "Flow and Thermal Structures in Heated Transitional Boundary Layers with and without Streamwise Acceleration," Ph.D. Dissertation, Dept. of Mech. Engr., Clemson University, Clemson, SC.

Keller, F.J., and Wang,T., 1993,"Effects of Criterion Functions on Intermittency in Heated Transitional Boundary Layers with and without Streamwise Acceleration," presented at the 1993 ASME International Gas Turbine and Aeroengine Congress, Cincinnati, OH.

Kistler, A.L., and Vrebalovich, T., 1966, "Grid Turbulence at Large Reynolds Numbers," *J. Fluid Mech.*, Vol.26, pp. 37-44.

Kuan, C.L., 1987, "An Experimental Investigation of Intermittent Behavior in the Transitional Boundary Layer," M.S Thesis, Dept. of Mech. Engr., Clemson University, Clemson, SC.

Kuan, C.L and Wang, T., 1990, "Investigation of Intermittent Behavior of Transitional Boundary Layer Using a Conditional Averaging Technique," *Experimental Thermal and Fluid Science*, Vol. 3, pp.157-170.

Mayle, R.E., 1991, "The Role of Laminar-Turbulent Transition in Gas Turbine Engines," *J. of Turbomachinery*, Vol.113, pp. 509-537.

Rued, K., and Wittig, S., 1985, "Free-Stream Turbulence and Pressure Gradient Effects on Heat Transfer and Boundary Layer Development on Highly Cooled Surfaces," *J. Engng. for Gas Turbines and Power*, Vol. 107, pp. 54-59.

Shome, B., 1991, "Development of a Three-wire Probe for the Measurement of Reynolds Stresses and Heat Fluxes in Transitional Boundary Layers," M.S. Thesis, Dept. of Mech. Engr., Clemson University.

Sohn, K.H., and Reshotko, E., 1991, "Experimental Study of Boundary Layer Transition With Elevated Freestream Turbulence on a Heated Flat Plate," NASA CR-187068.

Sohn, K.H., Reshotko, E., and Zaman, K.B.M.Q., 1991, "Experimental Study of Boundary Layer Transition on a Heated Flat Plate," ASME paper FED-Vol.114, pp.163-171.

Turner, A.B., 1971, "Local Heat Transfer Measurements on a Gas Turbine Blade," *J. Mech. Eng. Sci.*, Vol. 13, pp. 1-12.

Wang, T. and Simon, T.W., 1989, "Development of a Special-Purpose Test Surface Guided by Uncertainty Analysis," *Journal of Thermophysics*, Vol. 3, No. 1, pp.19-26.

Wang, T., Simon, T.W and Buddhavarapu, J., 1987, "Heat Transfer and Fluid Mechanics Measurements in Transitional Boundary Layer Flows," ASME *Journal of Turbomachinery*, Vol. 109, No.3, pp. 443-450.

Wang, T., Keller, F.J. and Zhou, D., 1992, "Experimental Investigation of Reynolds Shear Stresses and Heat Fluxes in a Transitional Boundary Layer," ASME HTD-Vol.226, *Fundamental and Applied Heat Transfer Research for Gas Turbine Engines*, pp. 61-70.

Wang, T., and Keller, F.J., 1993, "Favorable Pressure Gradient Effects on Boundary Layer Transition and Development of Flow and Thermal Structures," in preparation for publication.

Zhou, D., 1993, "Effects of Elevated Free-stream Turbulence and Streamwise Accelerations on Flow and Thermal Structures in Transitional Boundary Layers," Ph.D. Dissertation, Dept. of Mech. Engr., Clemson University.

Zhou, D., and Wang, T., 1992, "Laminar Boundary Layer Flow and Heat Transfer with Favorable Pressure Gradient at Constant K Values," ASME Paper 92-GT-246.

Zhou, D., and Wang, T., 1993, "Effects of Elevated Free-stream Turbulence on Flow and Thermal Structures in Transitional Boundary Layers," presented at the 1993 ASME International Gas Turbine and Aeroengine Congress, Cincinnati, OH.

Zhou, D., and Wang, T., 1993, "Combined Effects of Elevated Free-Stream Turbulence and Streamwise Acceleration on Flow and Thermal Structures in Transitional Boundary Layers," to be presented at the 1993 National Heat Transfer Conference at Atlanta, Georgia.

Table 1 Reynolds Numbers at Onset and End of Transition

(Baseline Case and Three Elevated FSTI Cases Without Acceleration)

		Baseline	G1K0	G2K0	G3K0
FSTI at X_S		0.5%	3.8%	5.5%	6.4%
U_∞ (m/s)		13.0	2.10	1.75	1.70
	x(cm)	61	45	45	42
Onset of	Re_x	5.0×10^5	6.0×10^4	5.0×10^4	4.5×10^4
Transition	$Re_{\delta*}$	1183	386	355	314
	Re_θ	434	161	148	131
	x(cm)	136	150	144	139
End of	Re_x	1.1×10^6	2.0×10^5	1.6×10^5	1.5×10^5
Transition	$Re_{\delta*}$	1947	735	659	608
	Re_θ	1327	480	404	375
	x(cm)	75	105	99	97
Length of	Re_x	6.0×10^5	1.4×10^5	1.1×10^5	1.0×10^5
Transition	$Re_{\delta*}$	764	349	304	294
	Re_θ	893	319	256	244

Table 2 Reynolds Numbers at Onset and End of Transition

(Four Accelerating Cases)

		G1K1	G1K2	G3K2	G3K3
FSTI at X_s		0.5%	3.8%	5.5%	6.4%
K x 10^{-6}		0.39	0.83	0.83	1
	x(cm)	62	77	47	62
Onset of	Re_x x 10^{-5}	0.9	1.2	0.7	0.8
Transition	$Re_{\delta*}$	489	505	414	425
	Re_θ	196	210	169	175
	x(cm)	182 ++	182 ++	182 ++	182 ++
End of	Re_x x 10^{-5}	5.0 +	6.0 +	8.5 +	11 +
Transition	$Re_{\delta*}$	1032 ++	901 ++	766 ++	568 ++
	Re_θ	681 ++	563 ++	453 ++	301 ++
	x(cm)	120 ++	105 ++	135 ++	120 ++
Length of	Re_x x 10^{-5}	4.1 +	4.8 +	7.8 +	10.2 +
Transition	$Re_{\delta*}$	543 ++	396 ++	352 ++	143 ++
	Re_θ	485 ++	353 ++	271 ++	119 ++

+ Data obtained from the extrapolation of Stanton number distributions

++ Data obtained st Station 12 when transition is not completed.

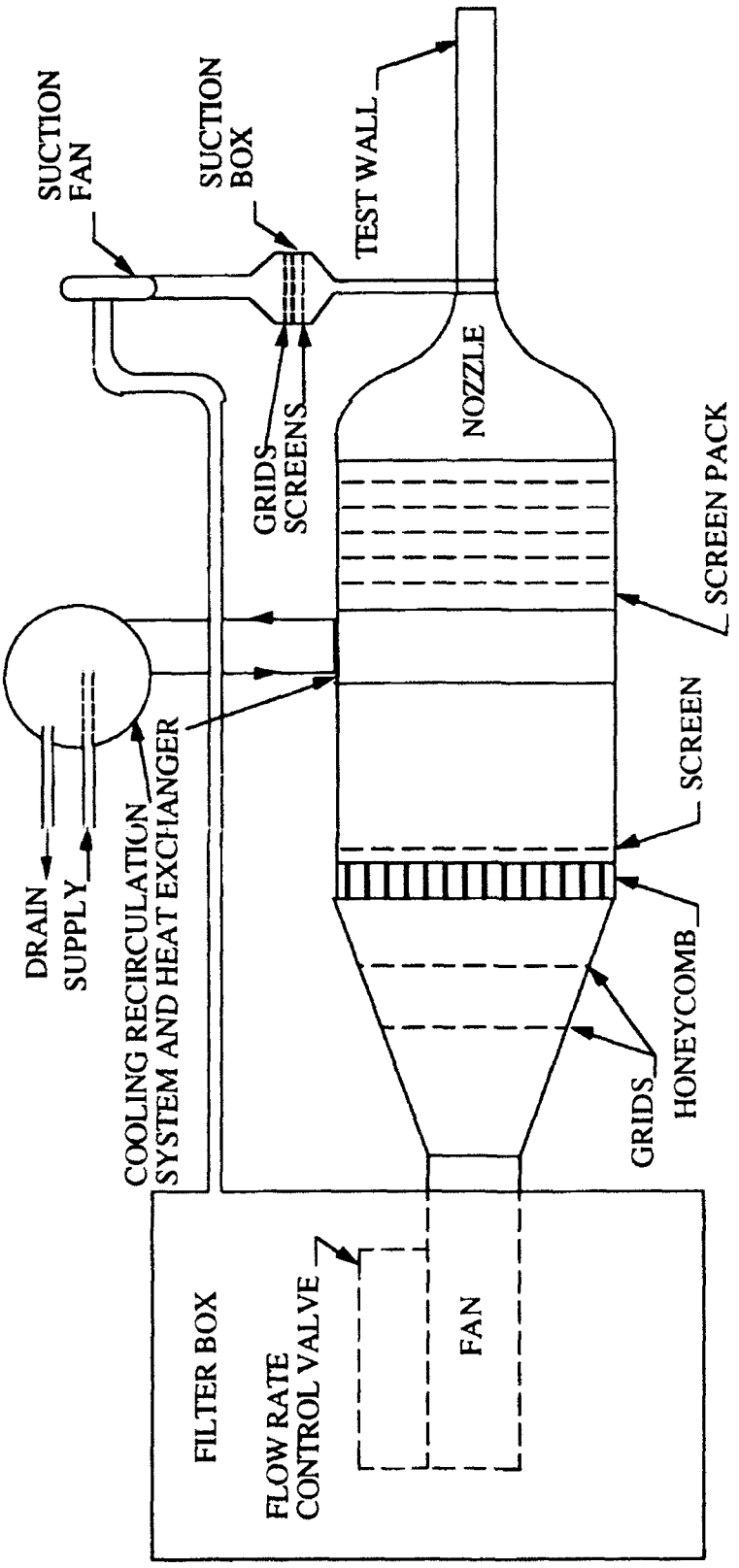

Fig. 1 Schematic of wind tunnel facility.

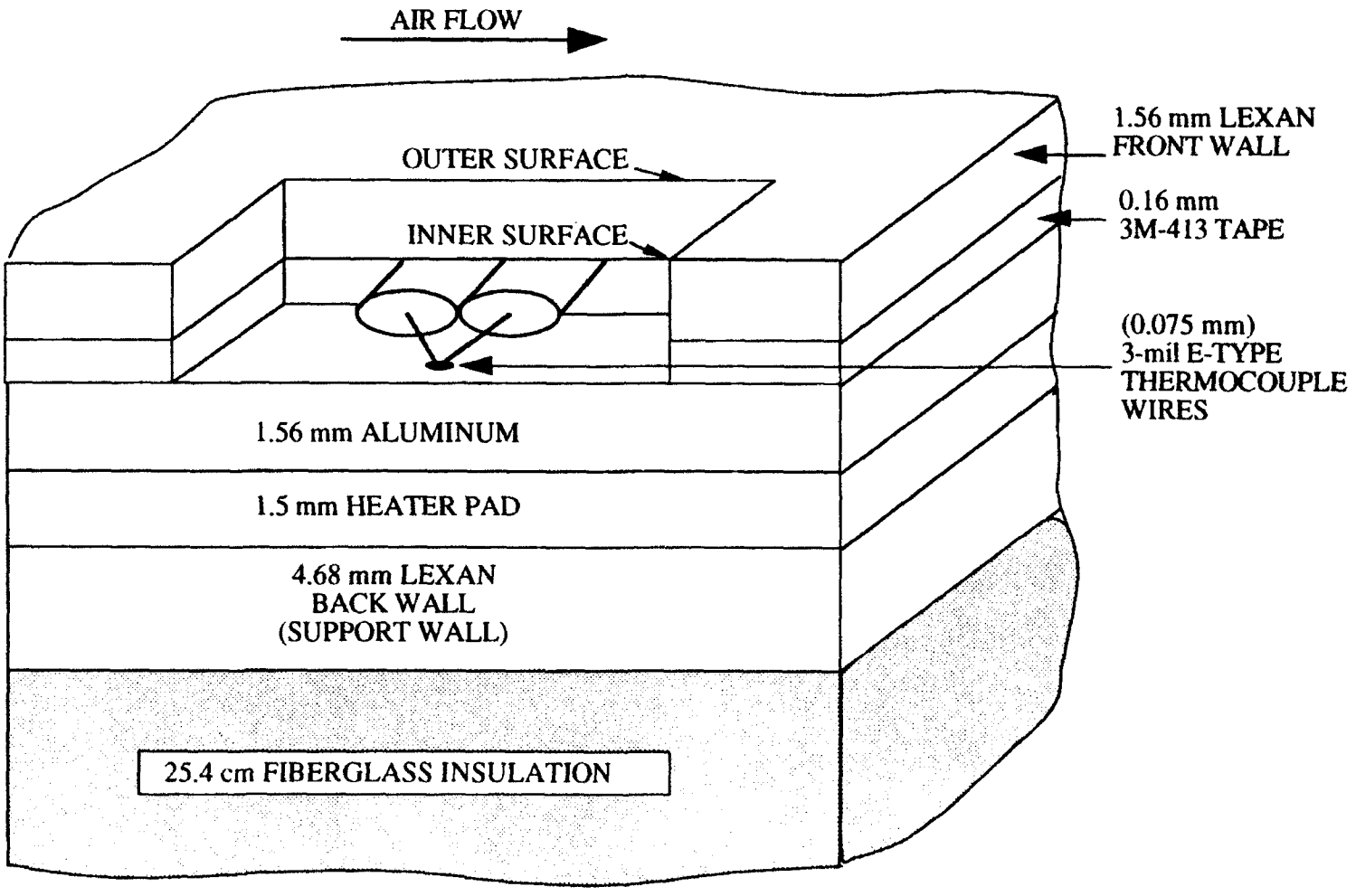

Fig. 2 Schematic of composite heated test wall.

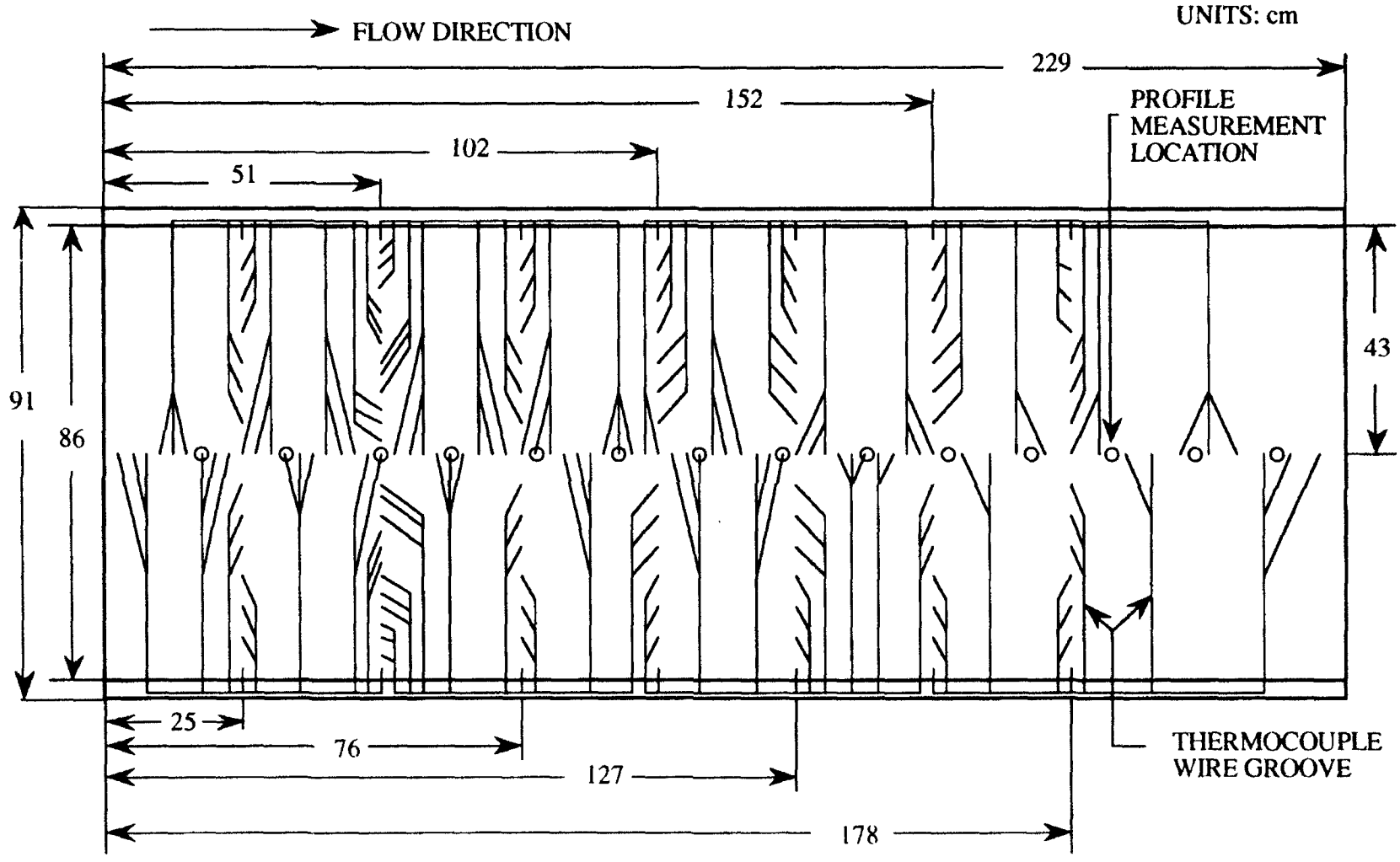

Fig. 3 Schematic of thermocouple layout. o - indicates location for boundary layer measurements.

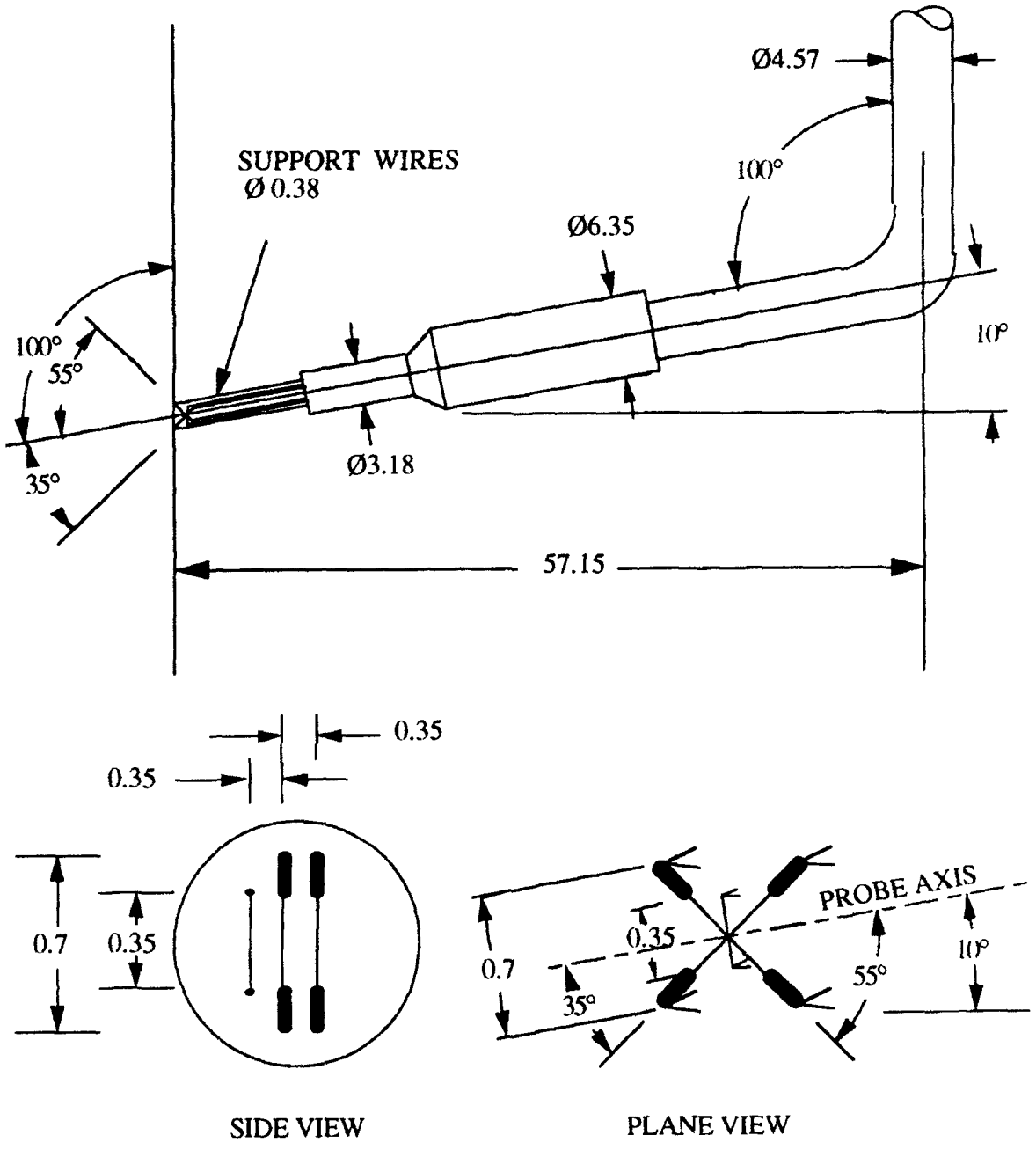

DIMENSIONS IN mm

Fig. 5 3-wire boundary layer sensor for measuring Reynolds stresses and heat fluxes.

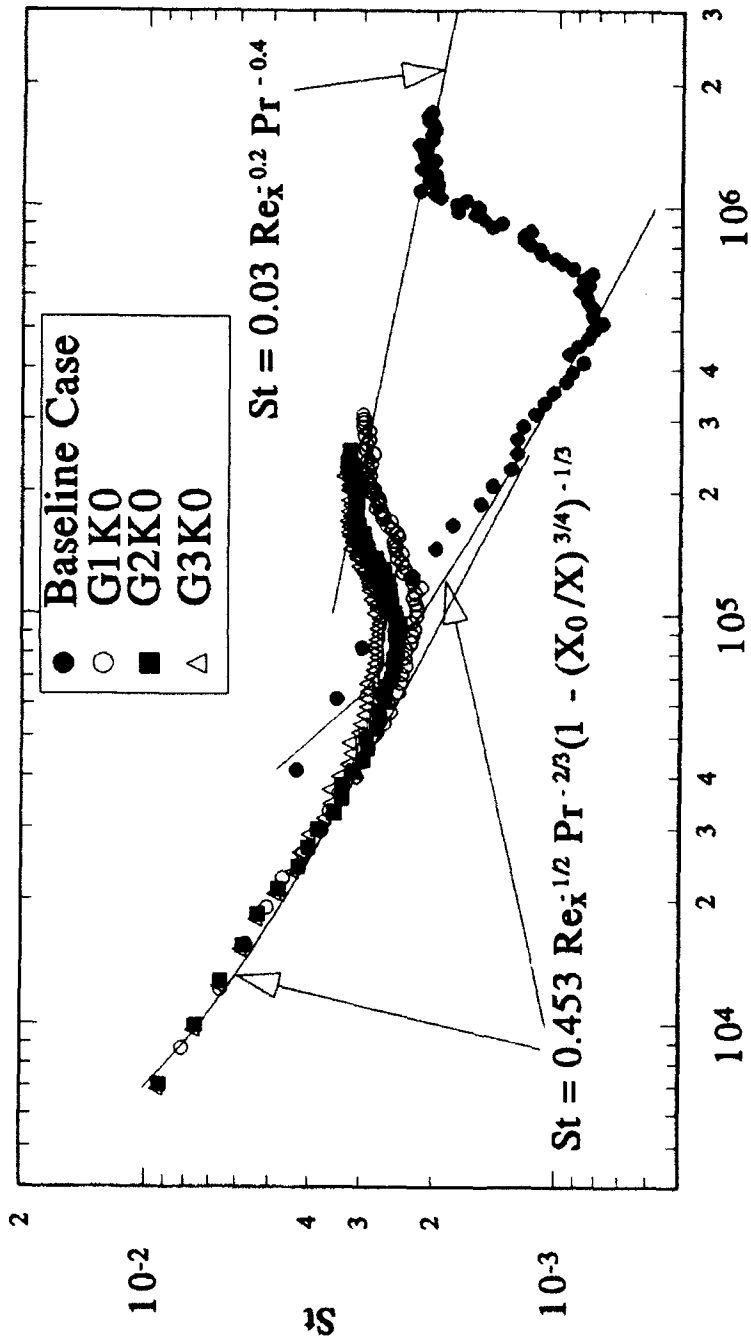

Fig. 6 Stanton Number Distributions (zero acceleration)

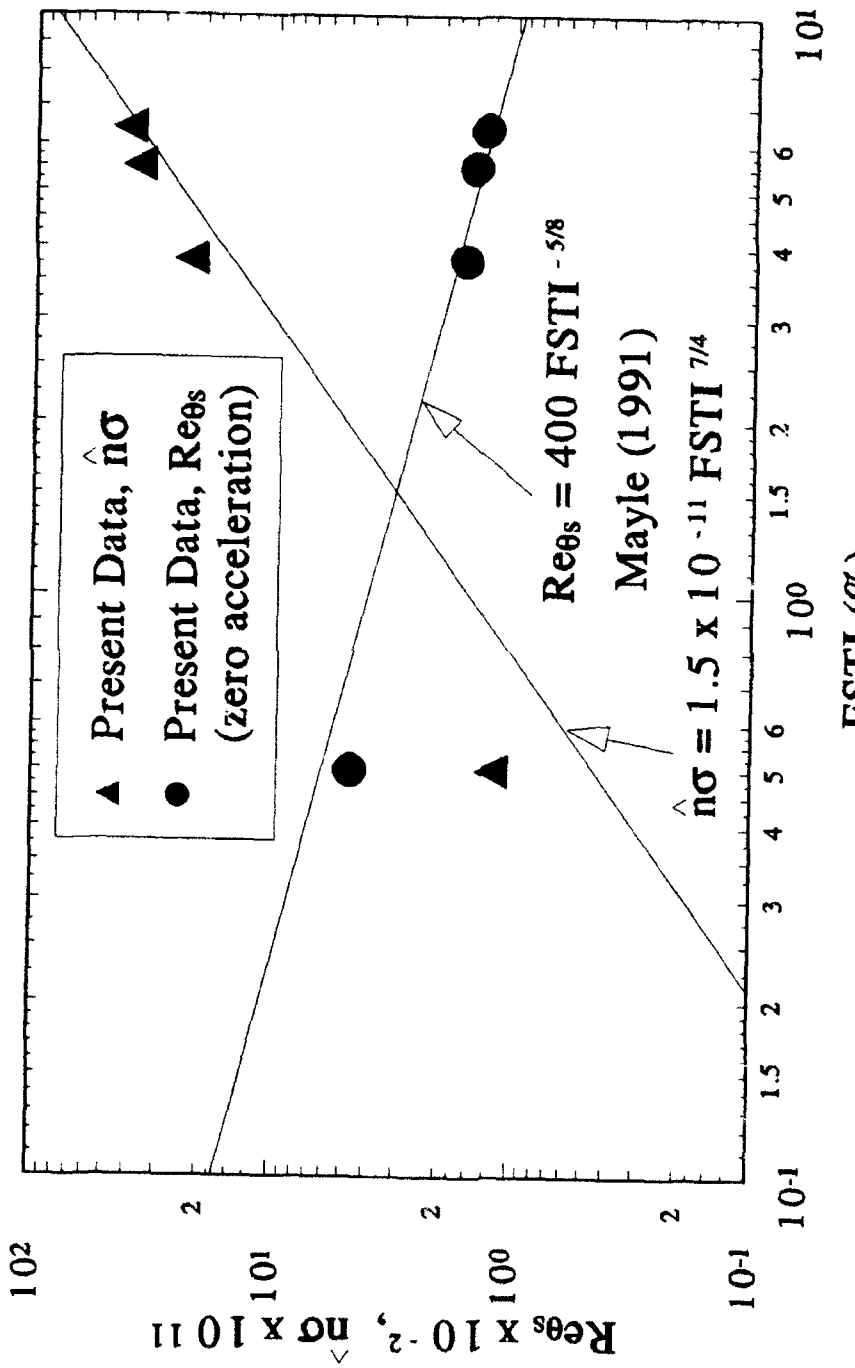

Fig. 7 Onset of Transition & Turbulent Spot Formation Rate

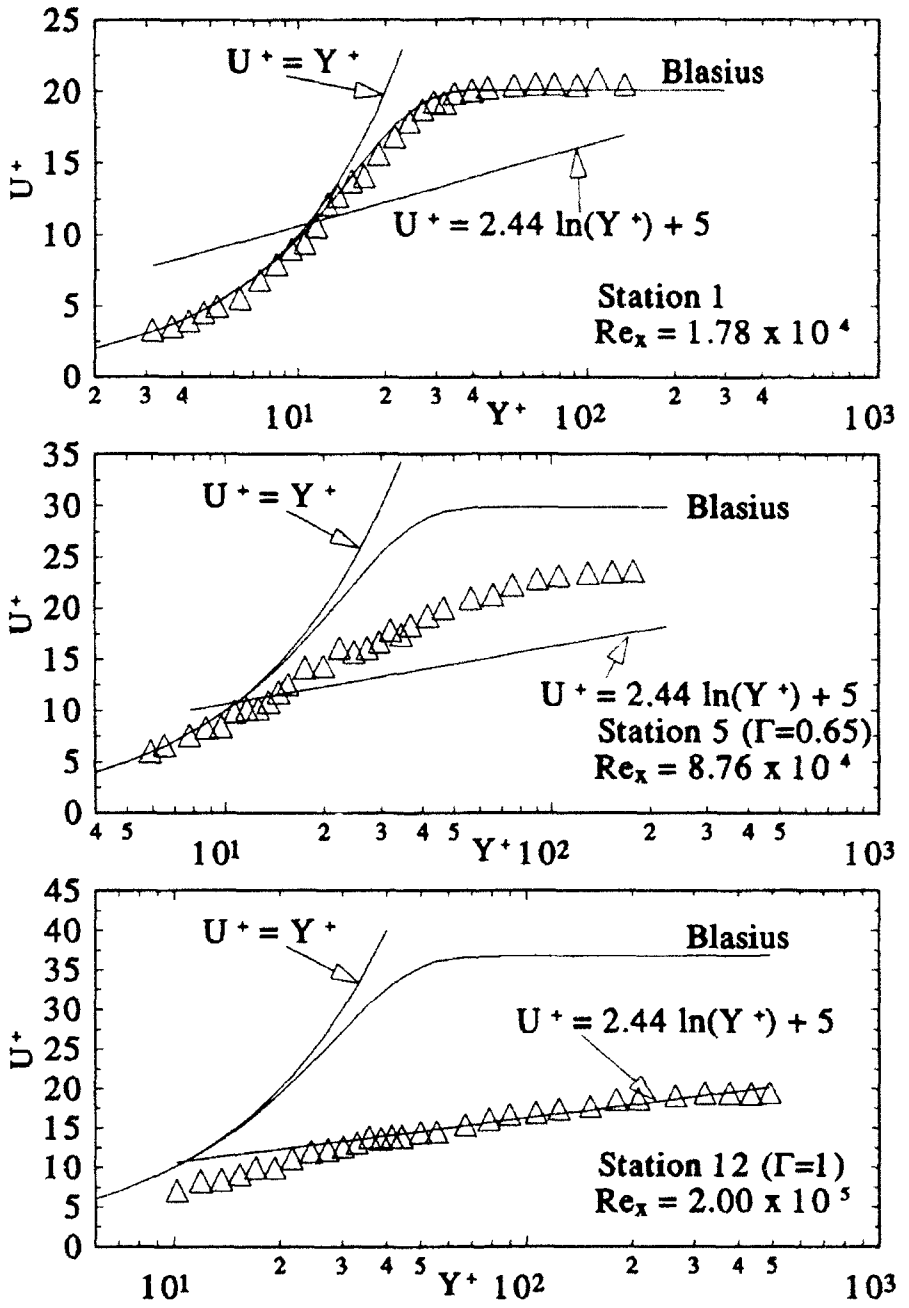

Fig. 8 Mean Velocity Profiles for G2K0 Case

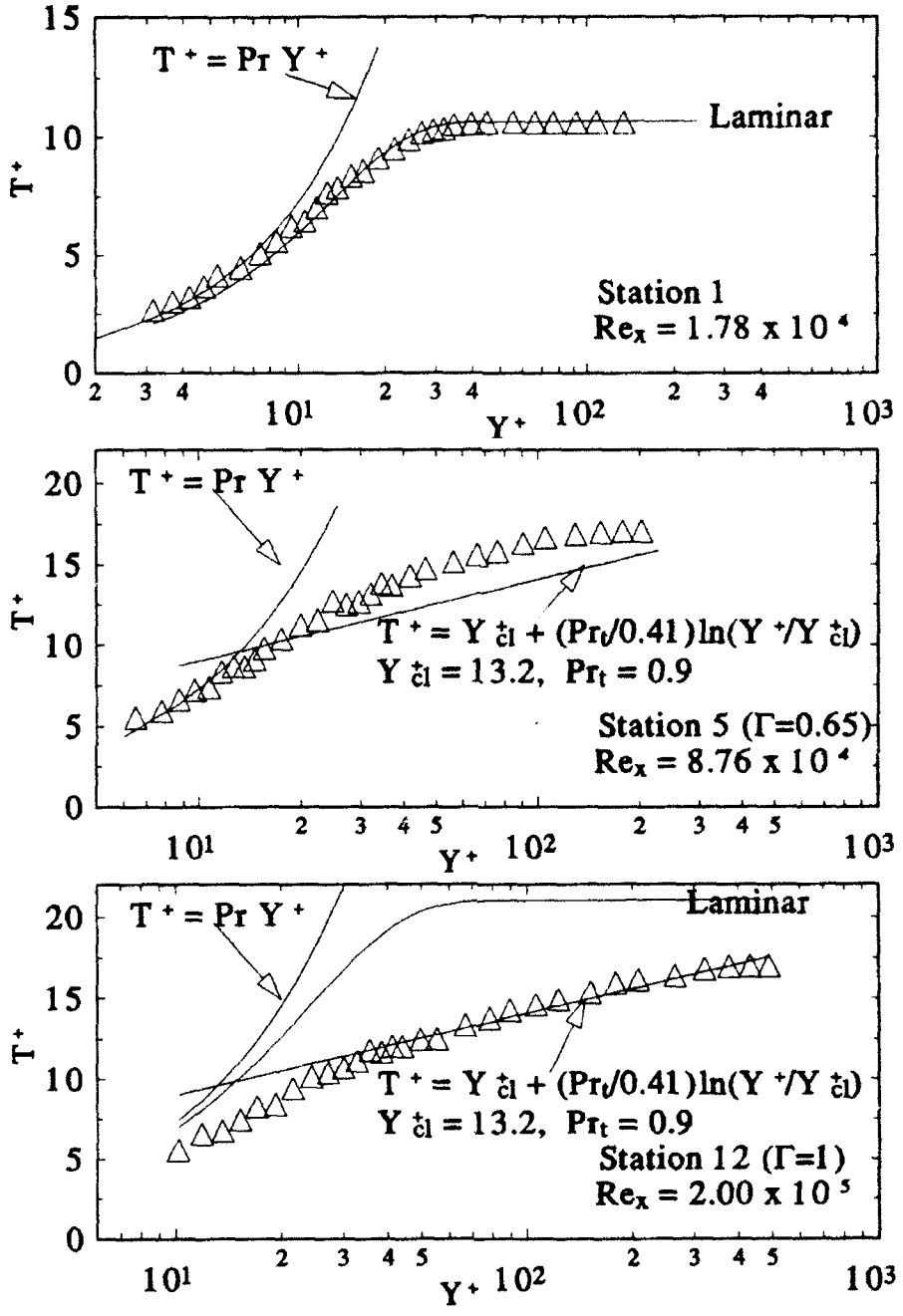

Fig. 9 Mean Temperature Profiles for G2K0 Case

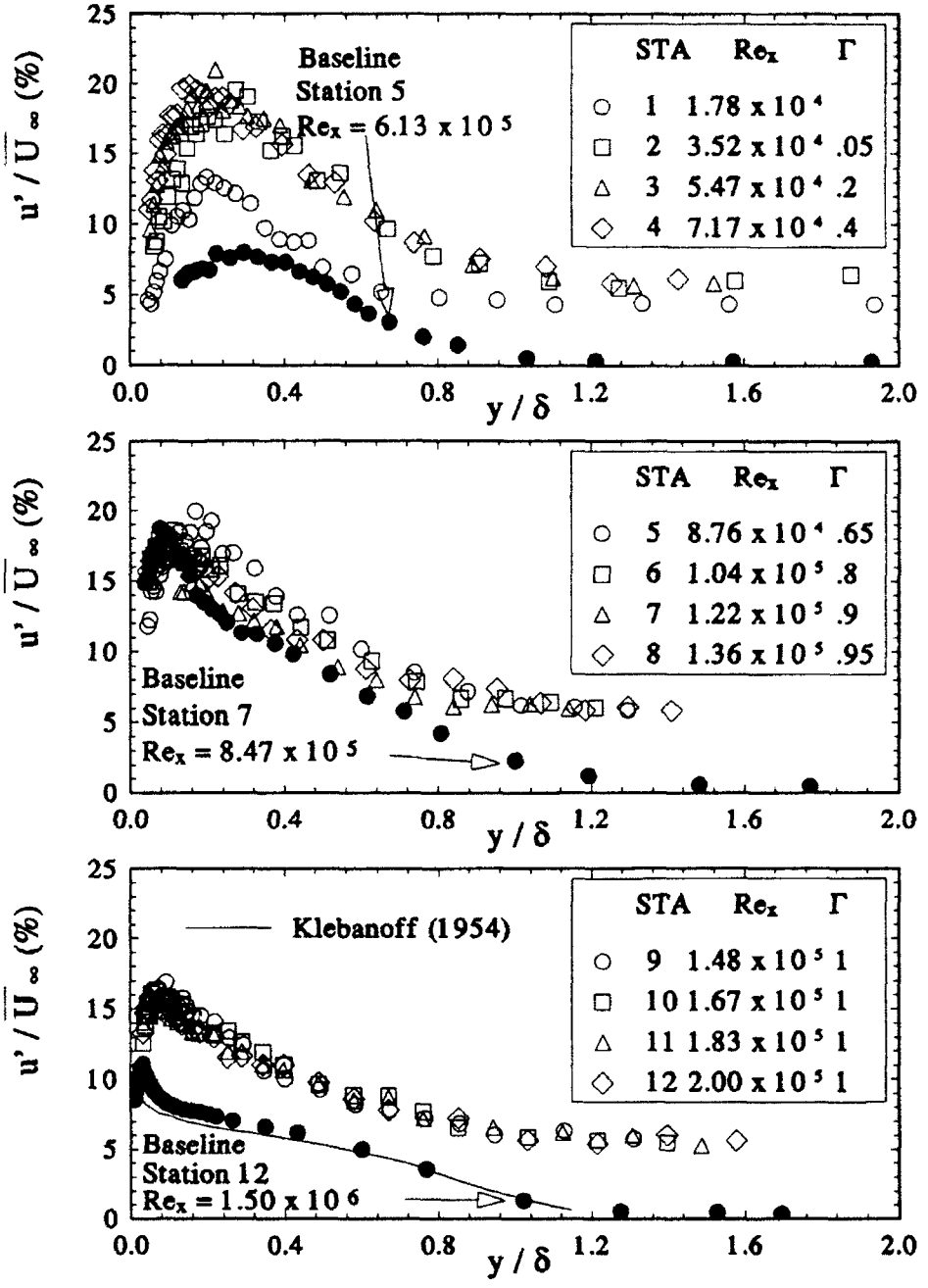

Fig. 10 Streamwise Reynolds Normal Stress Profiles for G2K0 Case

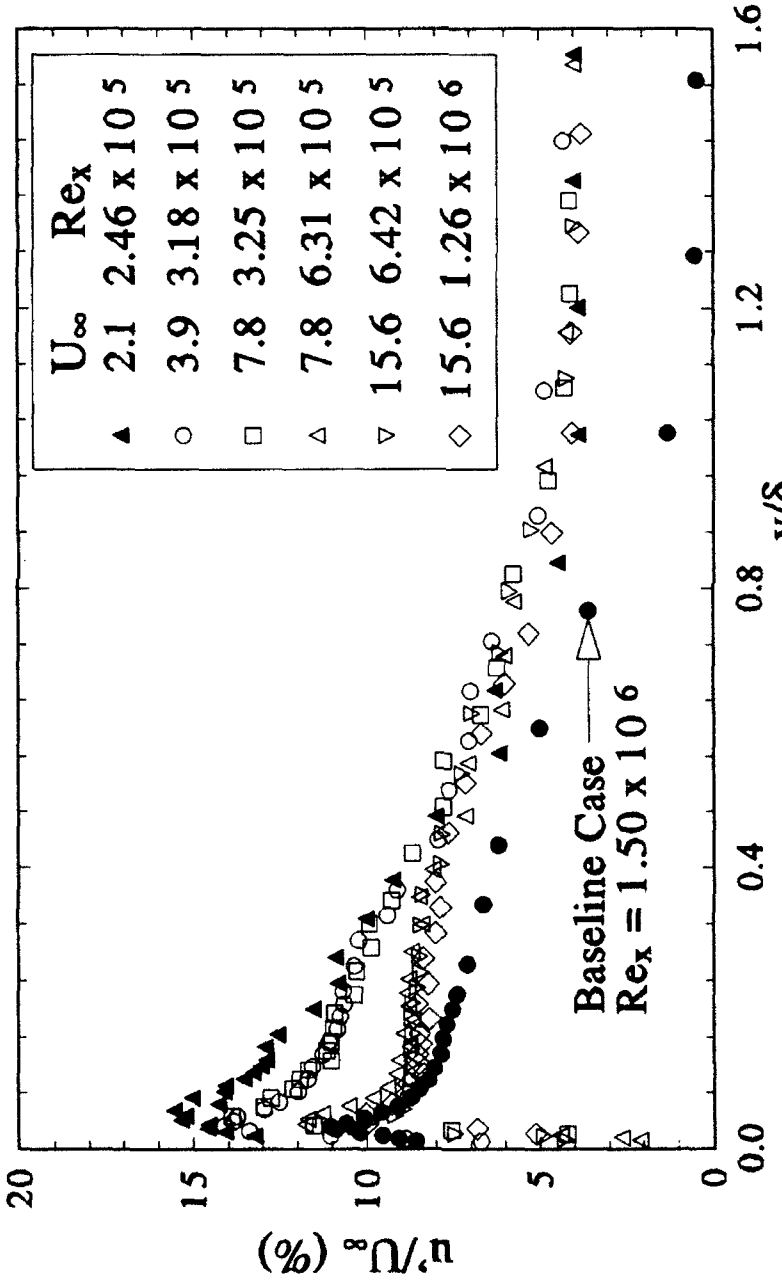

Fig. 11 Low Reynolds Number Effect on u' Distribution

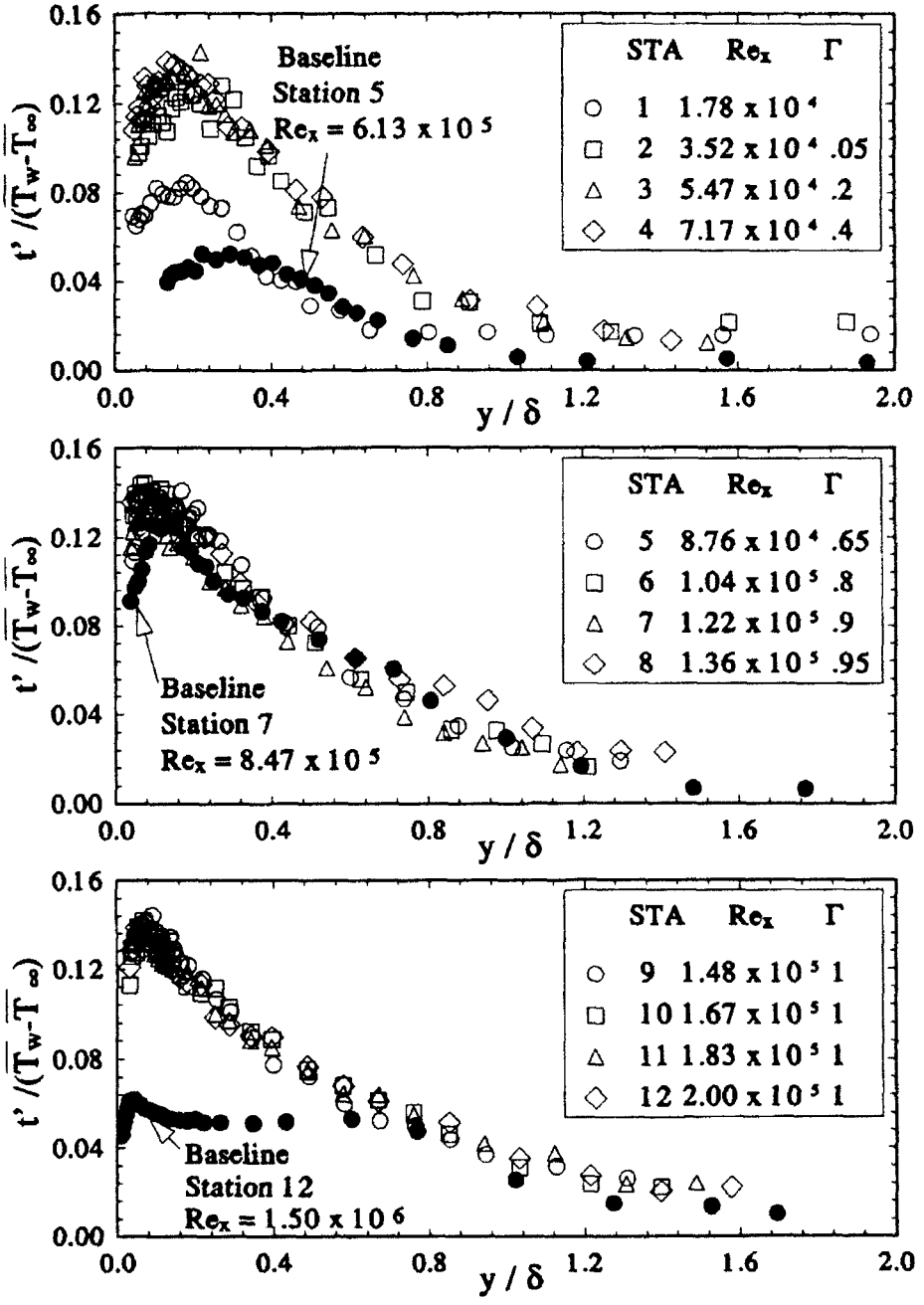

Fig. 12 RMS Temperature Profiles for G2K0 Case

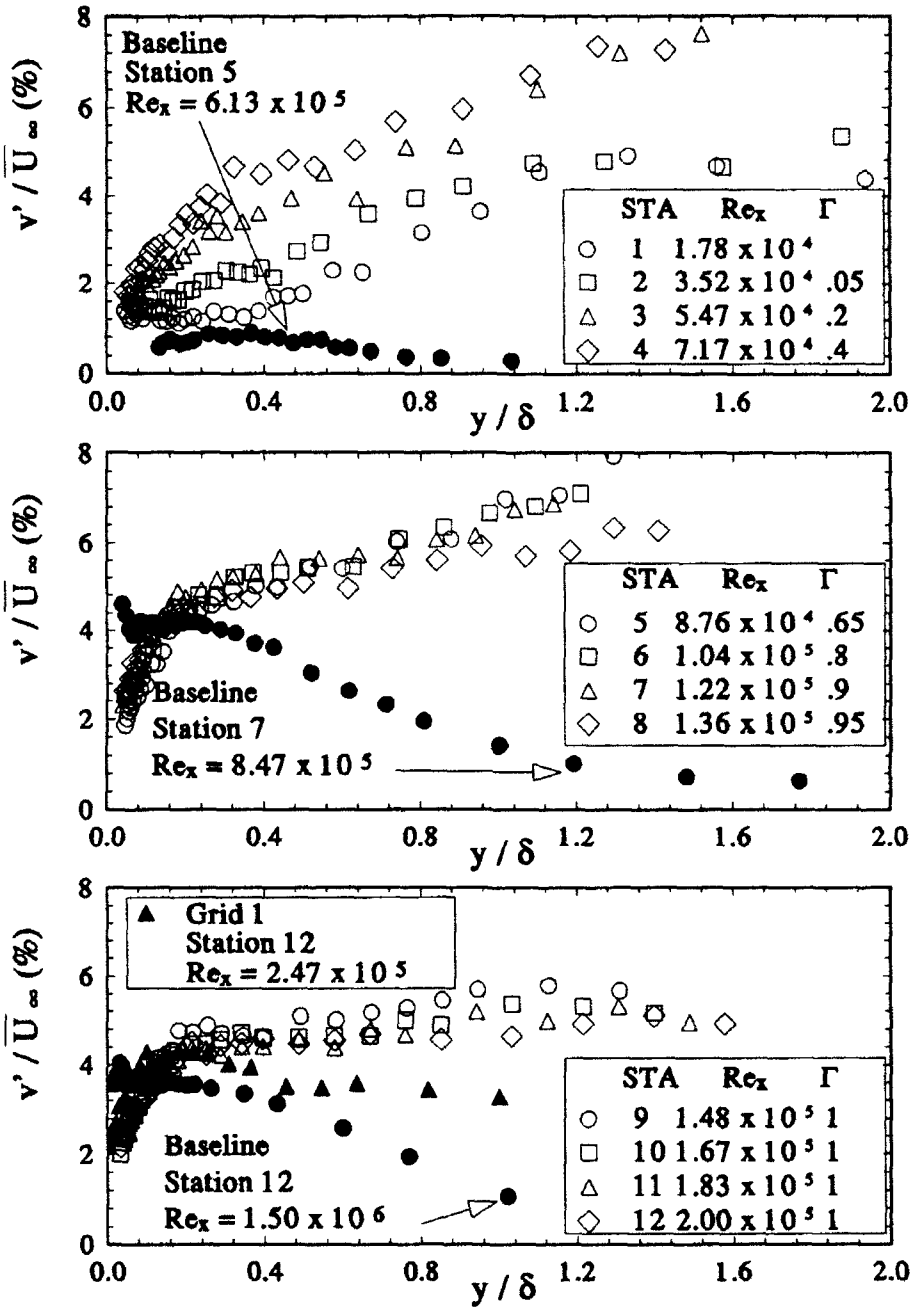

Fig. 13 Cross-tream Reynolds Normal Stress Profiles for G2K0 Case

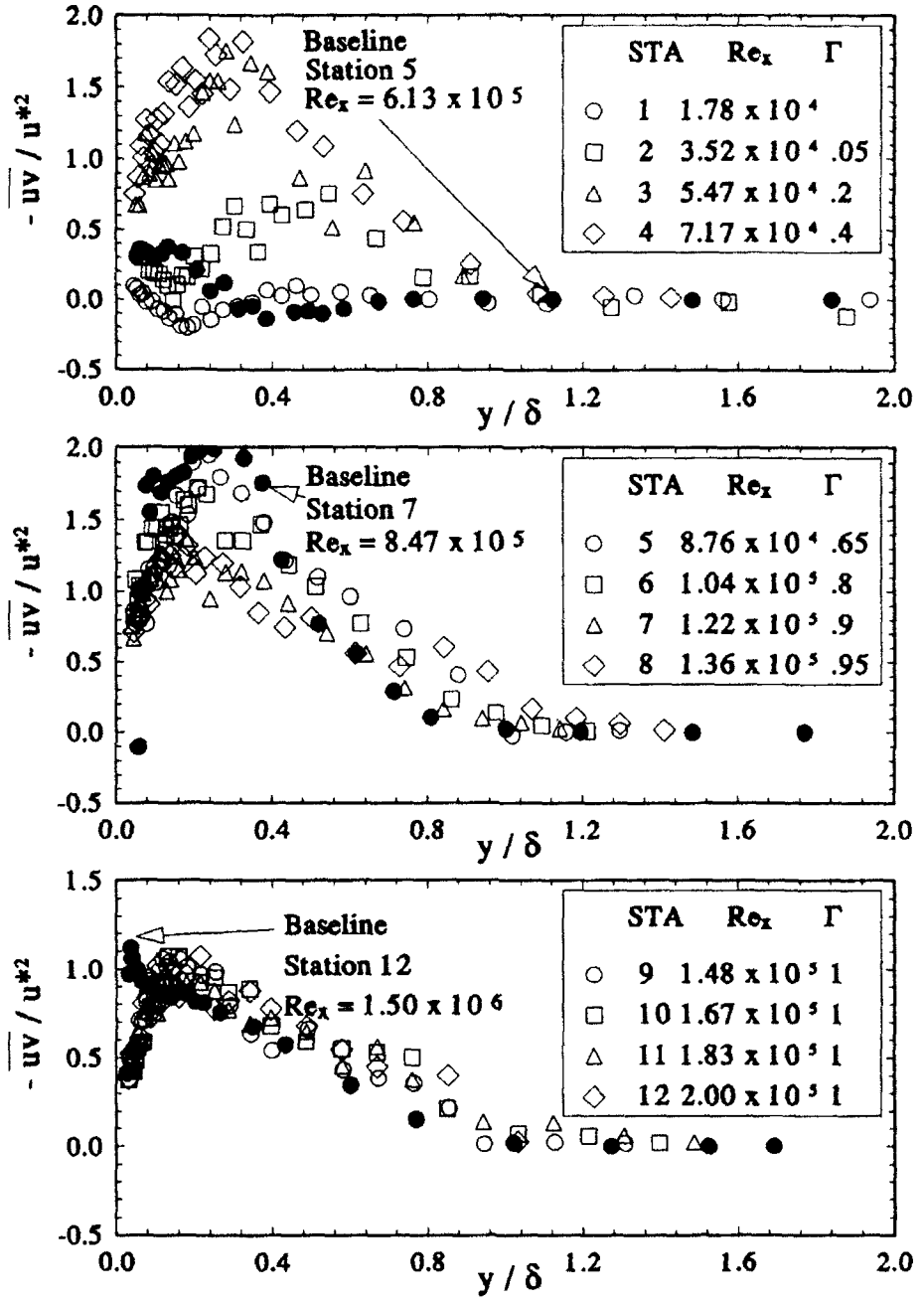

Fig. 14 Reynolds Shear Stress Distributions for G2K0 Case

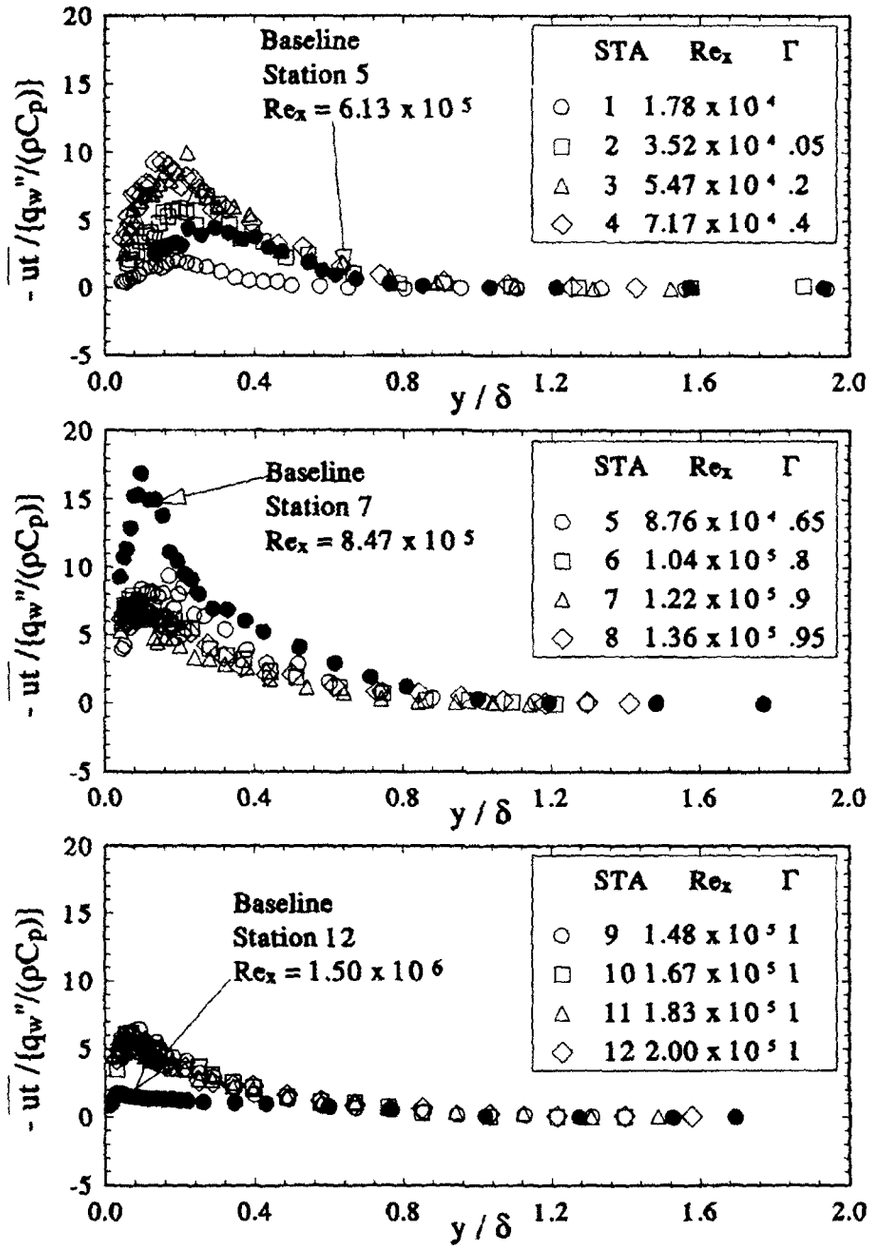

Fig. 15 Streameise Reynolds Heat Flux Distributions for G2K0 Case

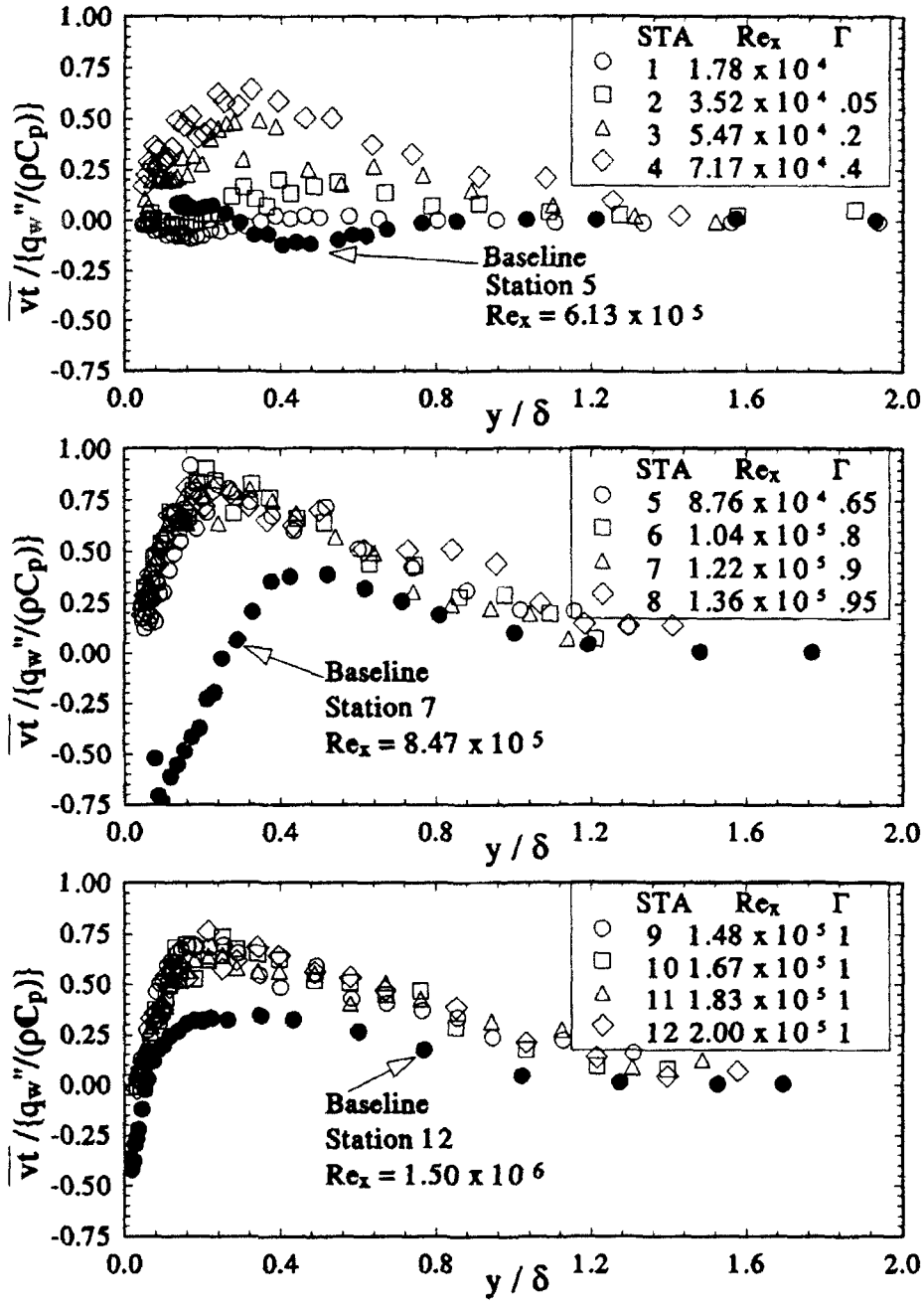

Fig. 16 Cross-stream Reynolds Heat Flux Distributions for G2K0 Case

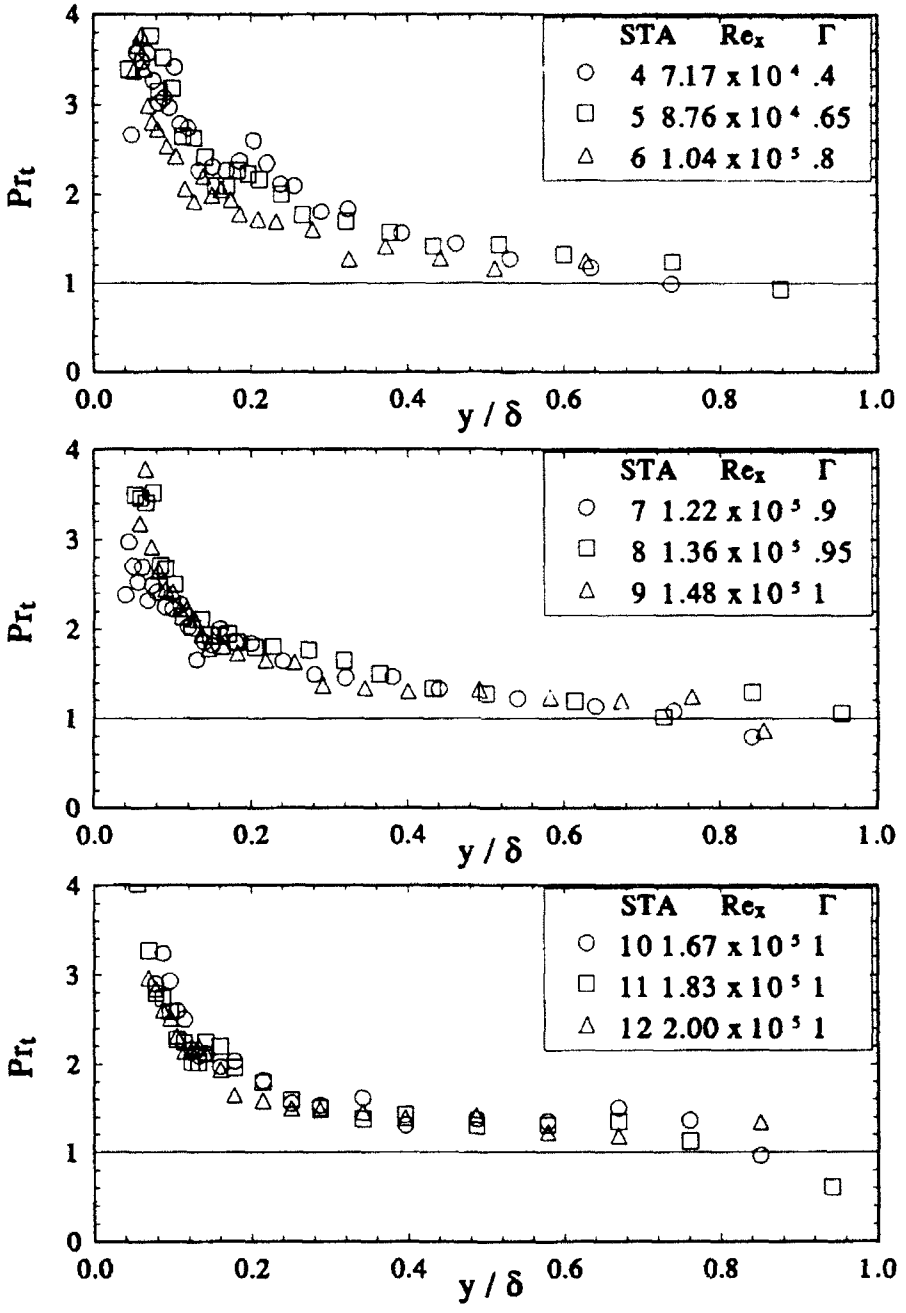

Fig. 17 Turbulent Prandtl Number Distributions for G2K0 Case (Note: The baseline case results are not shown in this figure because of the controversial and unresolved issure of negative Pr_t)

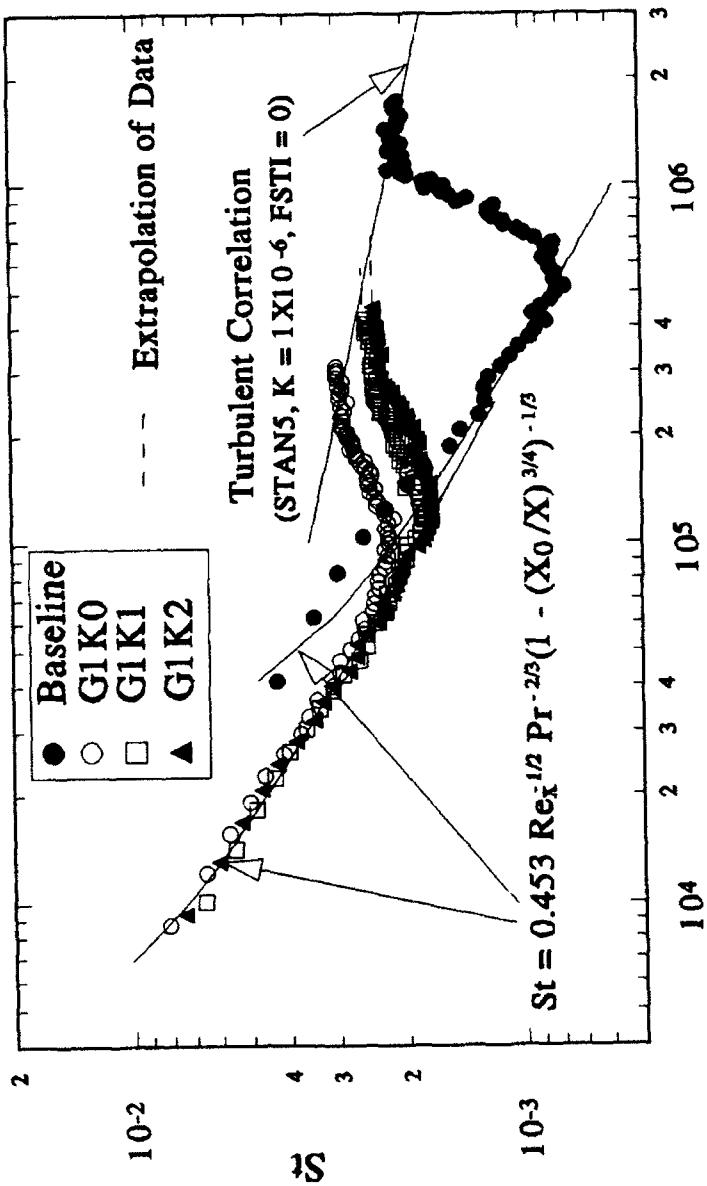

Fig. 18 Stanton Number Distributions for Grid 1

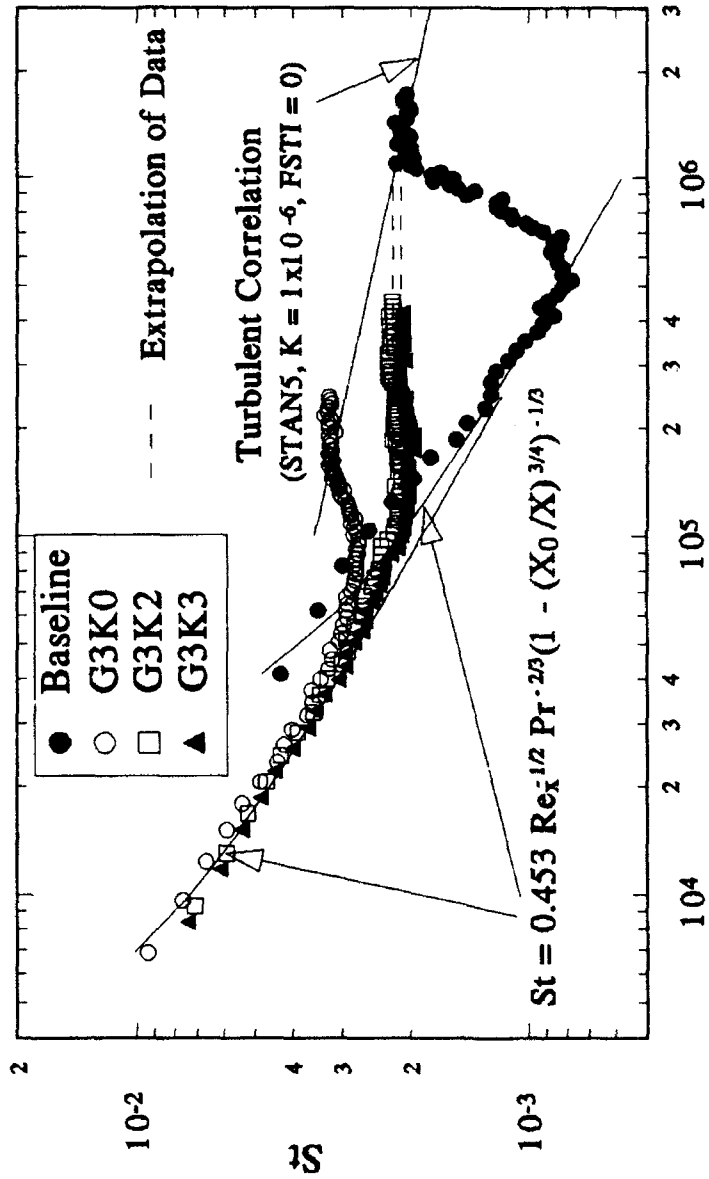

Fig. 19 Stanton Number Distributions for Grid 3

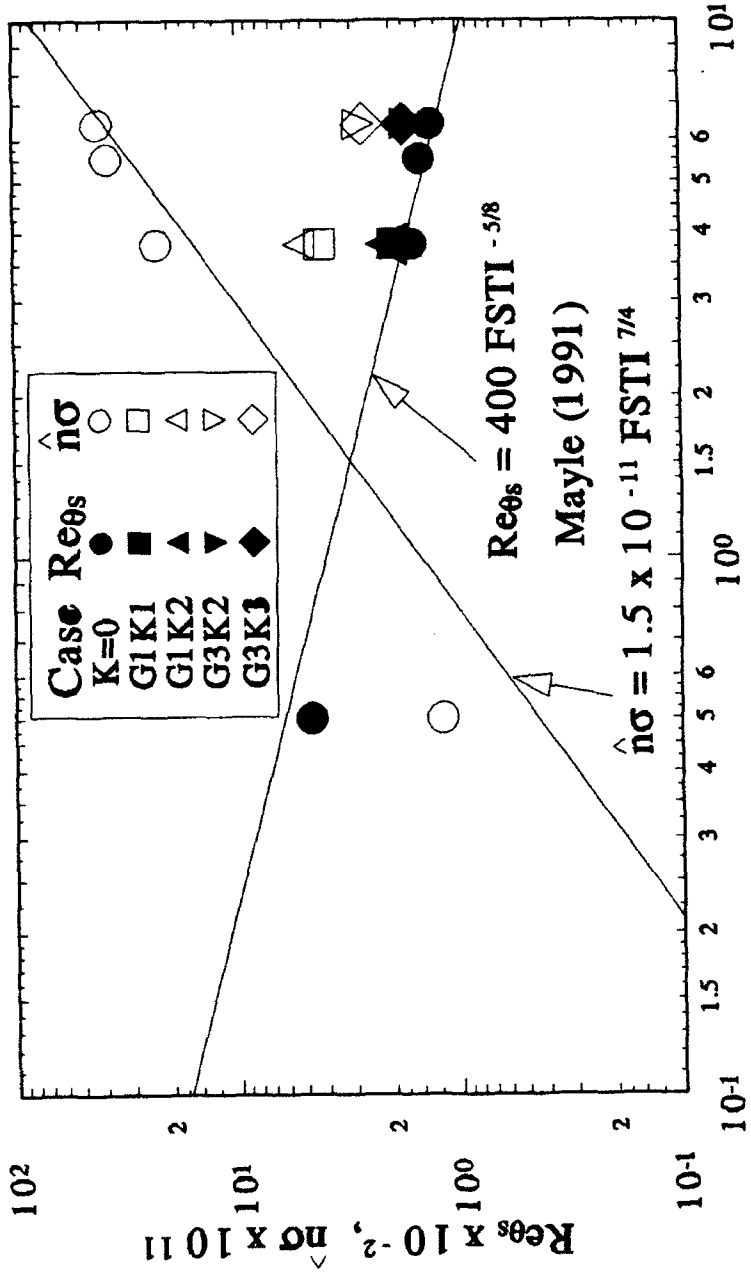

Fig. 20 Transition Onset and Turbulent Spot Formation Rate

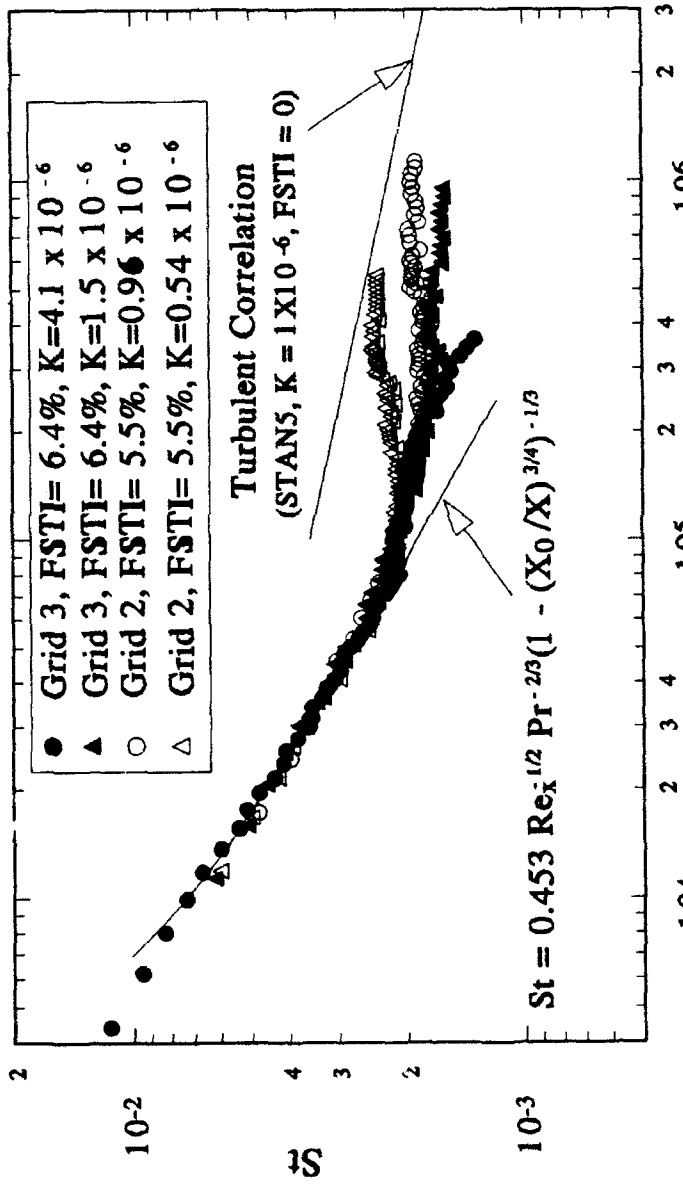

Fig. 21 Stanton Number Distributions for Grid 3 & 2

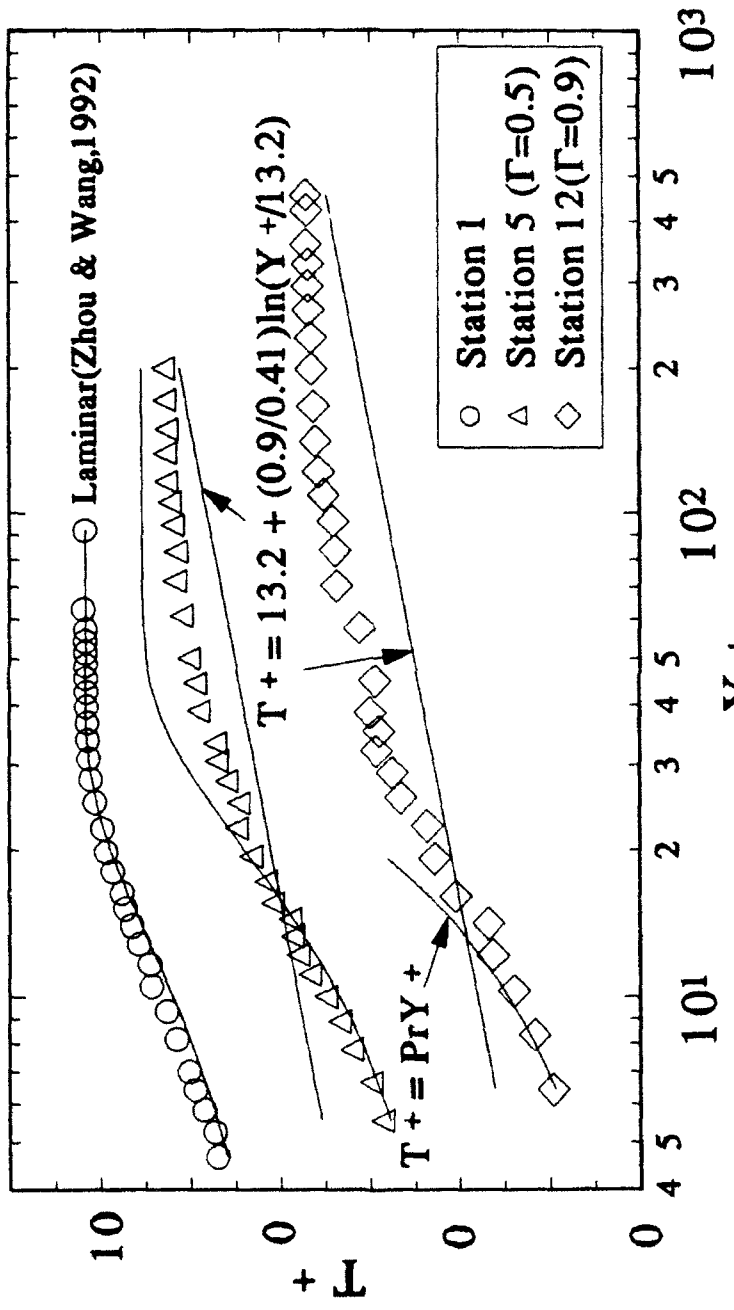

Fig. 22 Mean Temperature Profiles for G3K3 Case

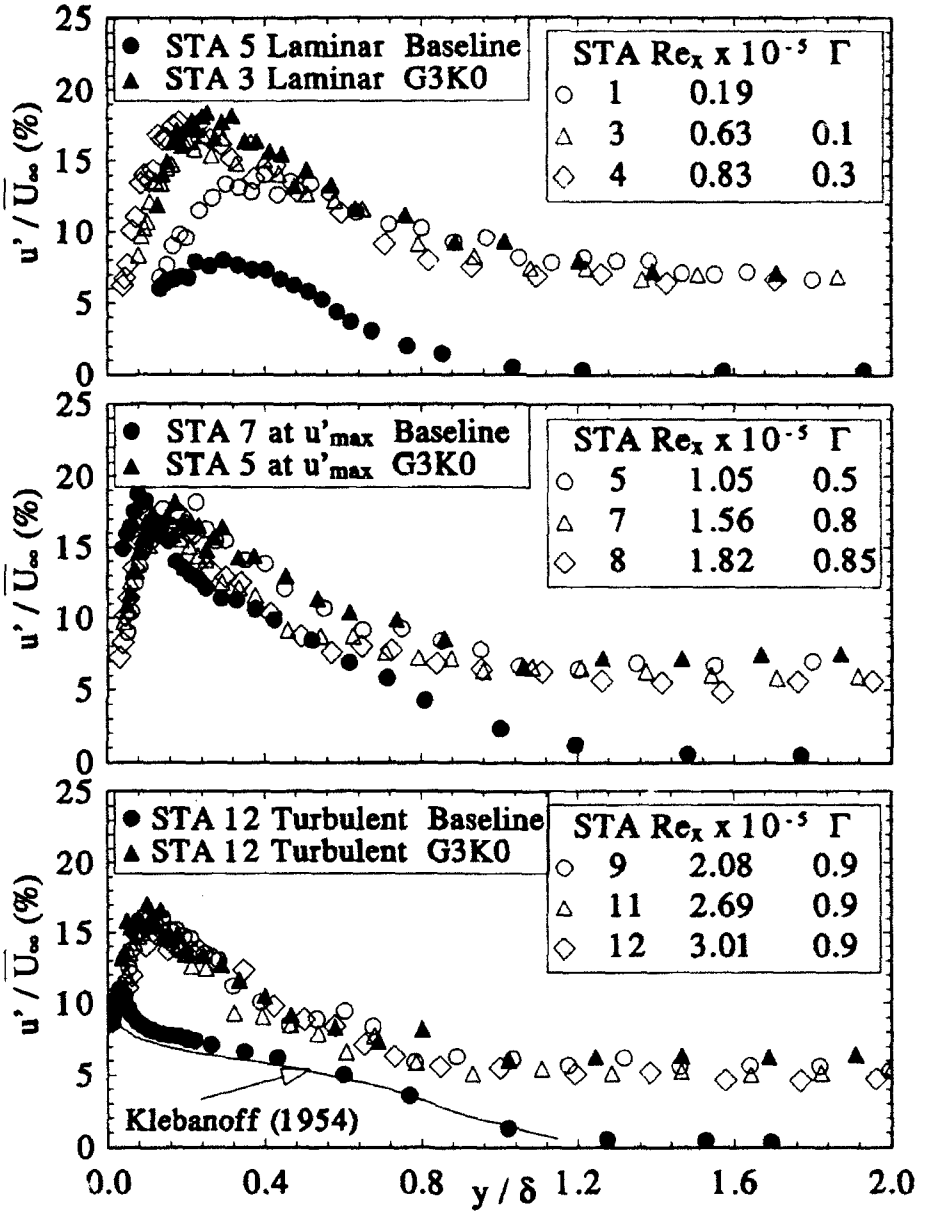

Fig. 23 Streamwise Reynolds Normal Stress Profiles for G3K3 Case

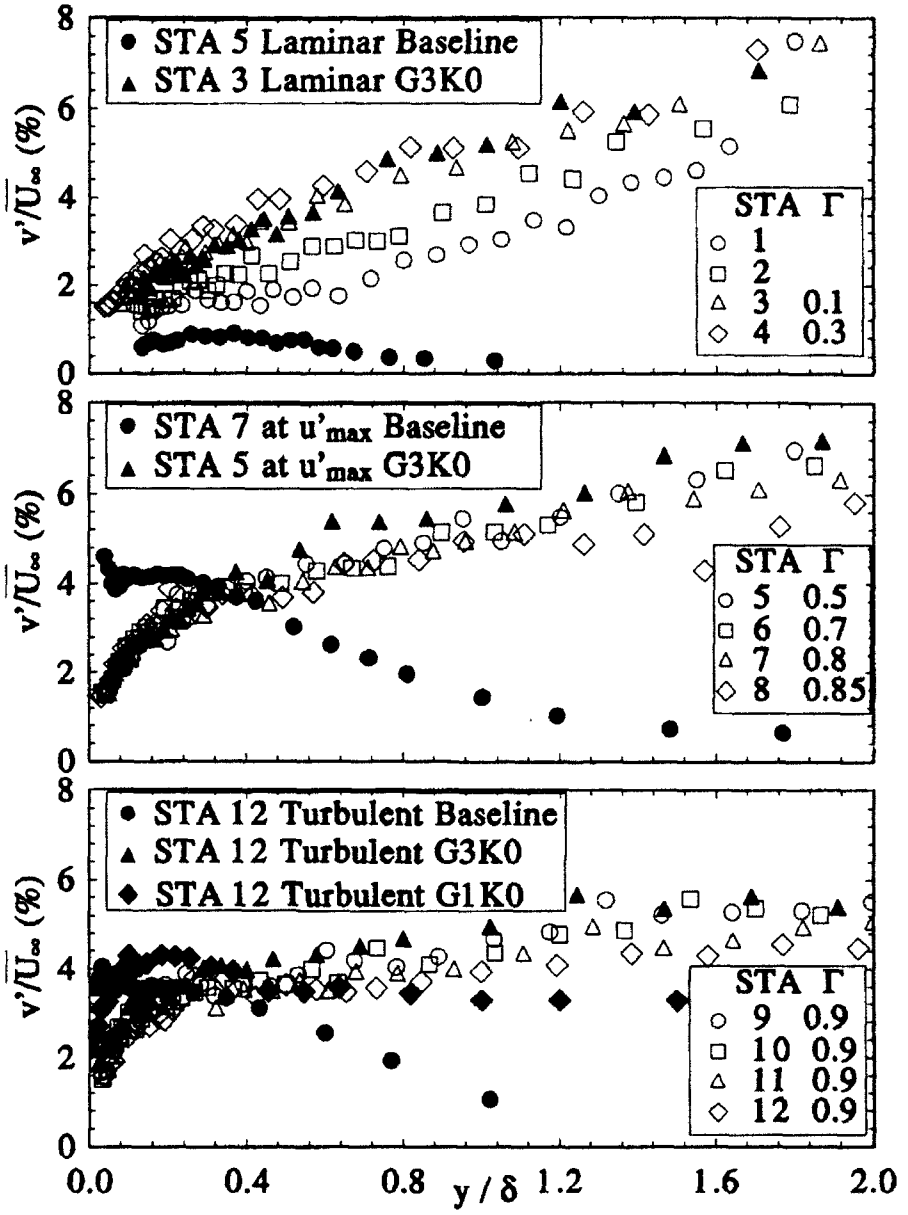

Fig. 24 Cross-Stream Reynolds Normal Stress Profiles for G3K3 Case

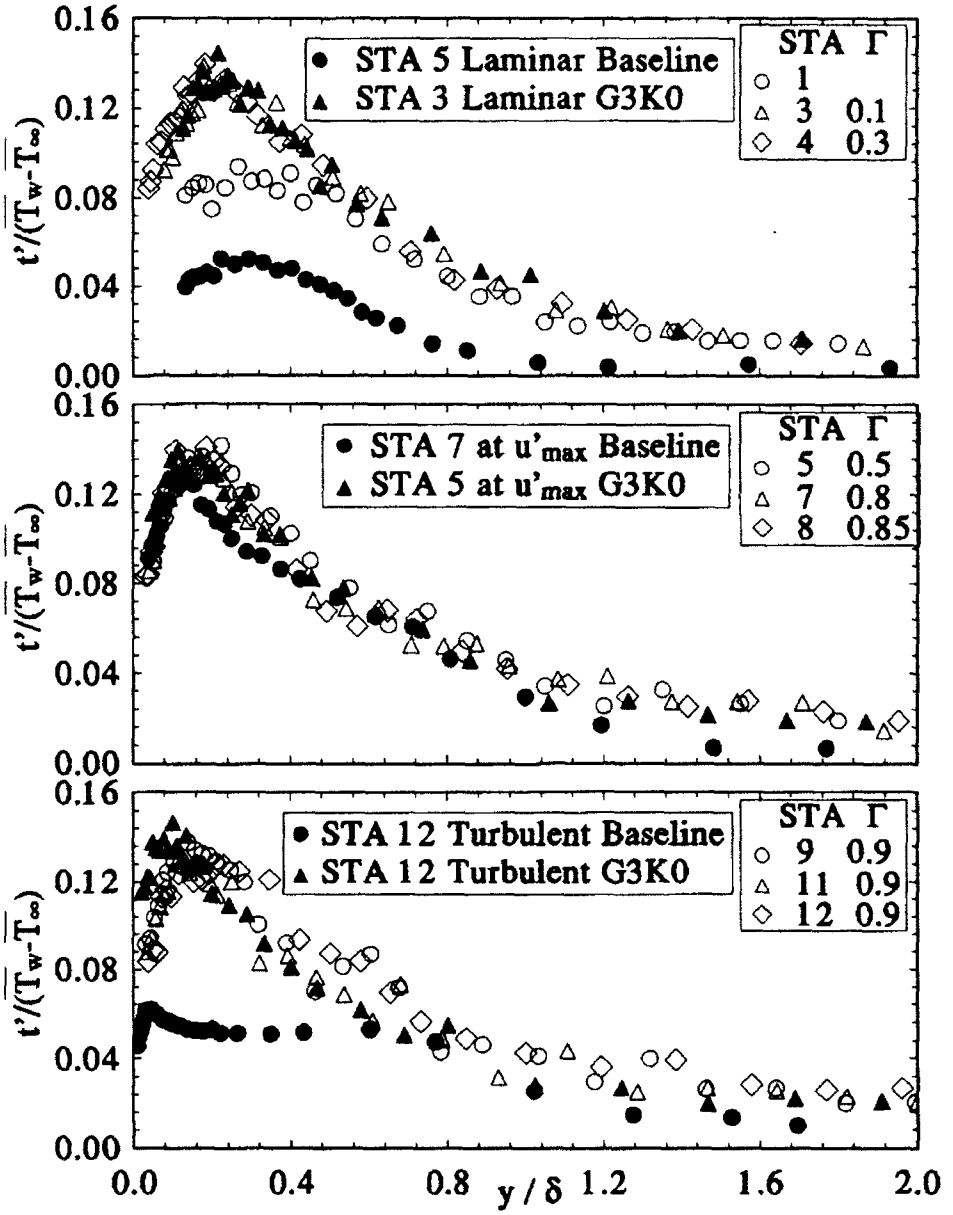

Fig. 25 Streamwise Evolution of t' Profiles for G3K3 Case

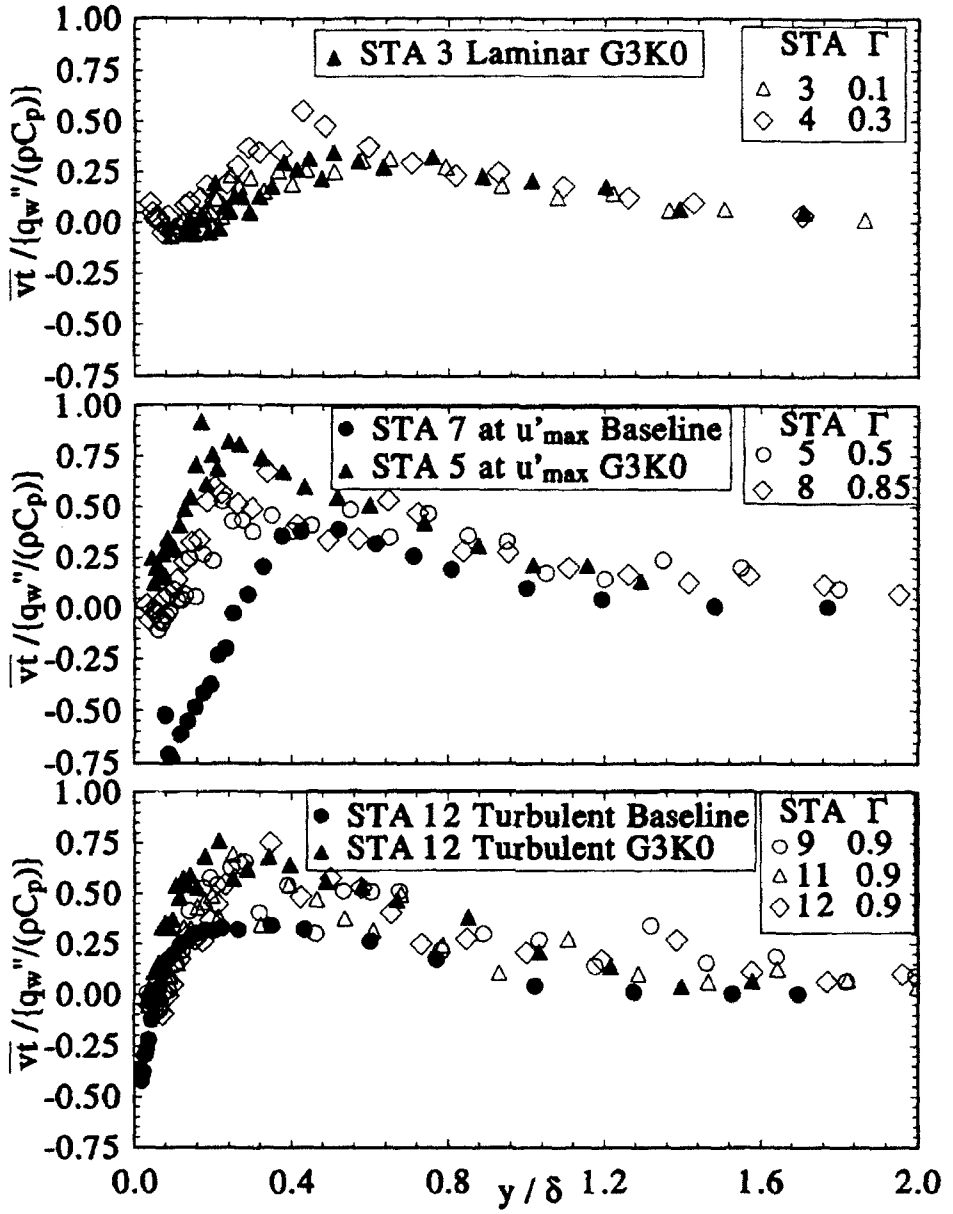

Fig. 26 Cross-Stream Reynolds Heat Flux Distribution for G3K3 Case

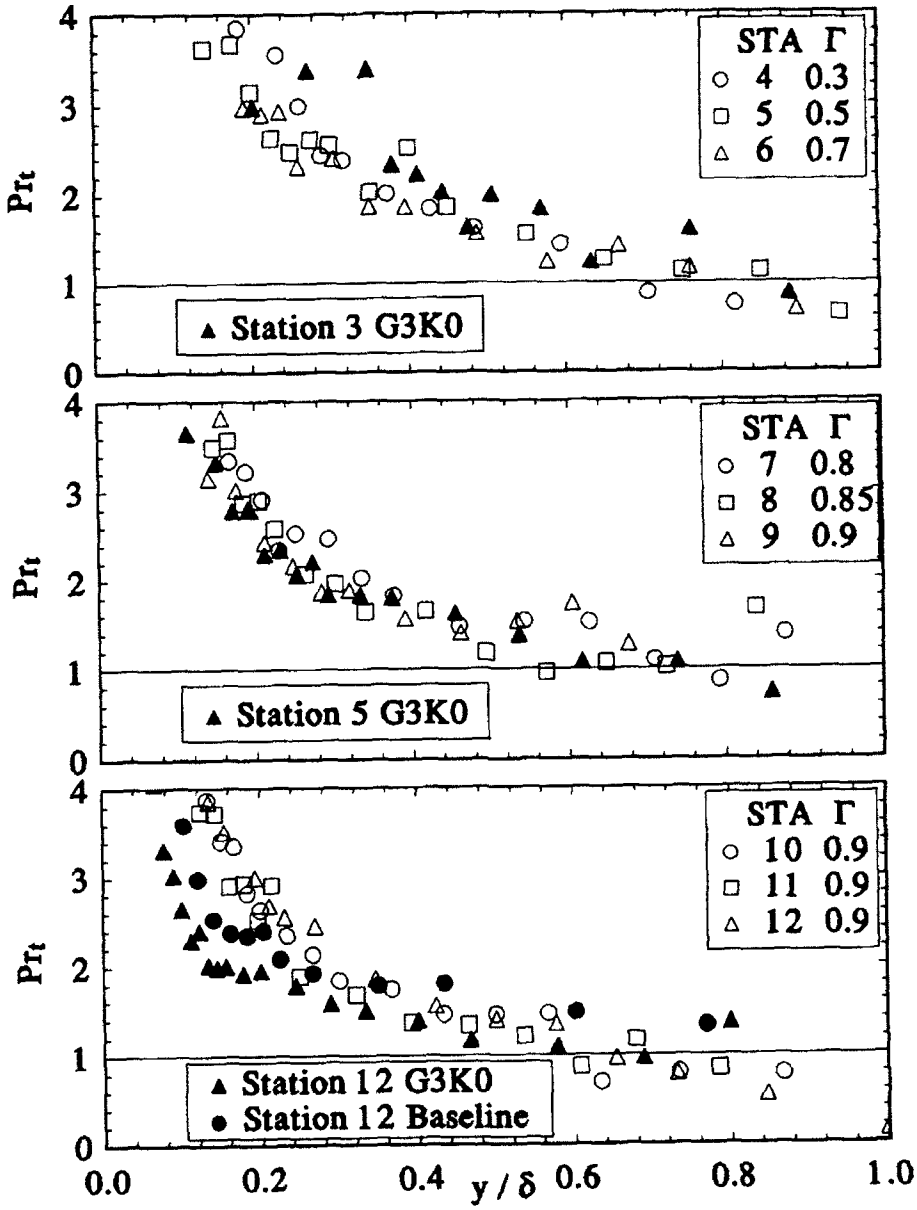

Fig. 27 Turbulent Prandtl Number Distribution for G3K3 Case

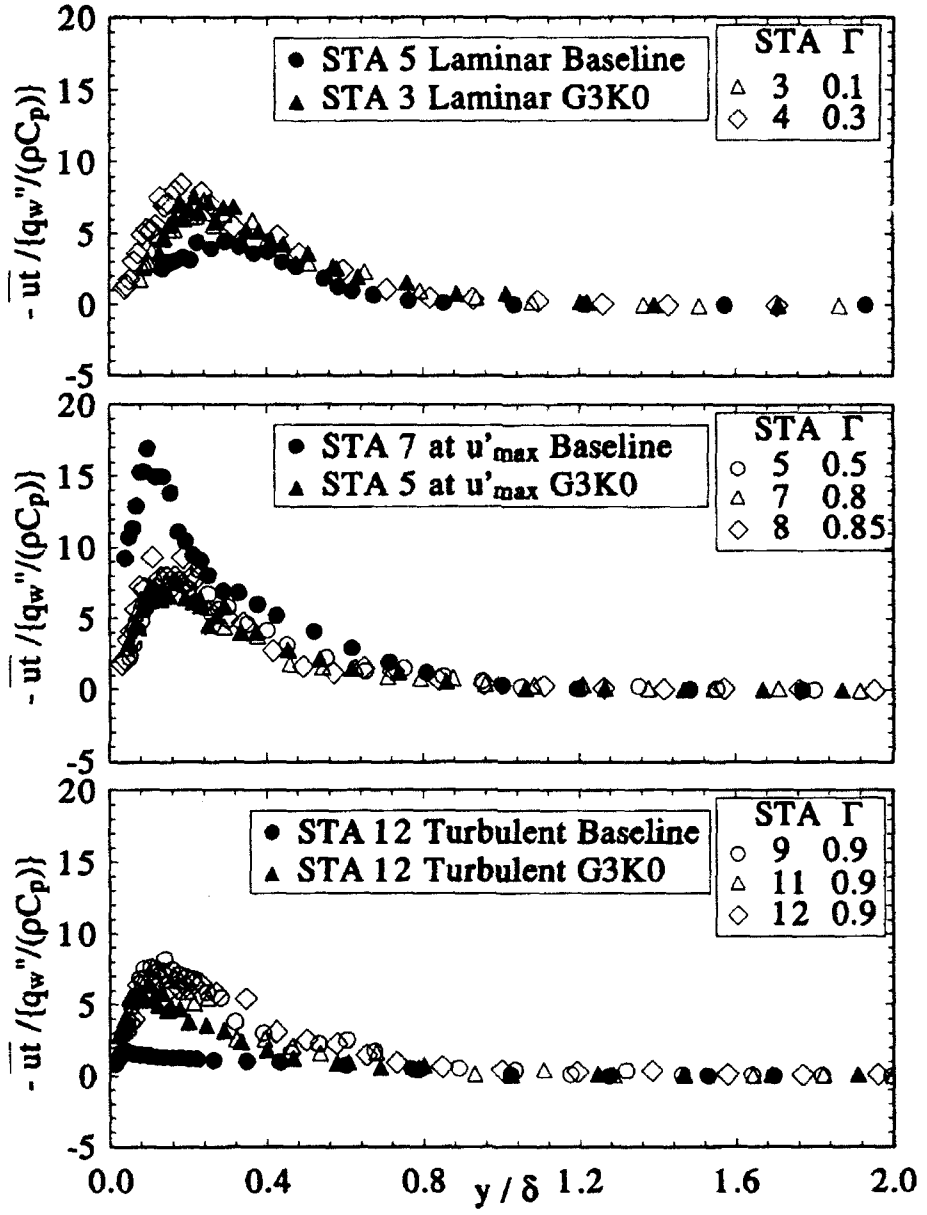

Fig. 28 Streamwise Reynolds Heat Flux Distribution for G3K3 Case

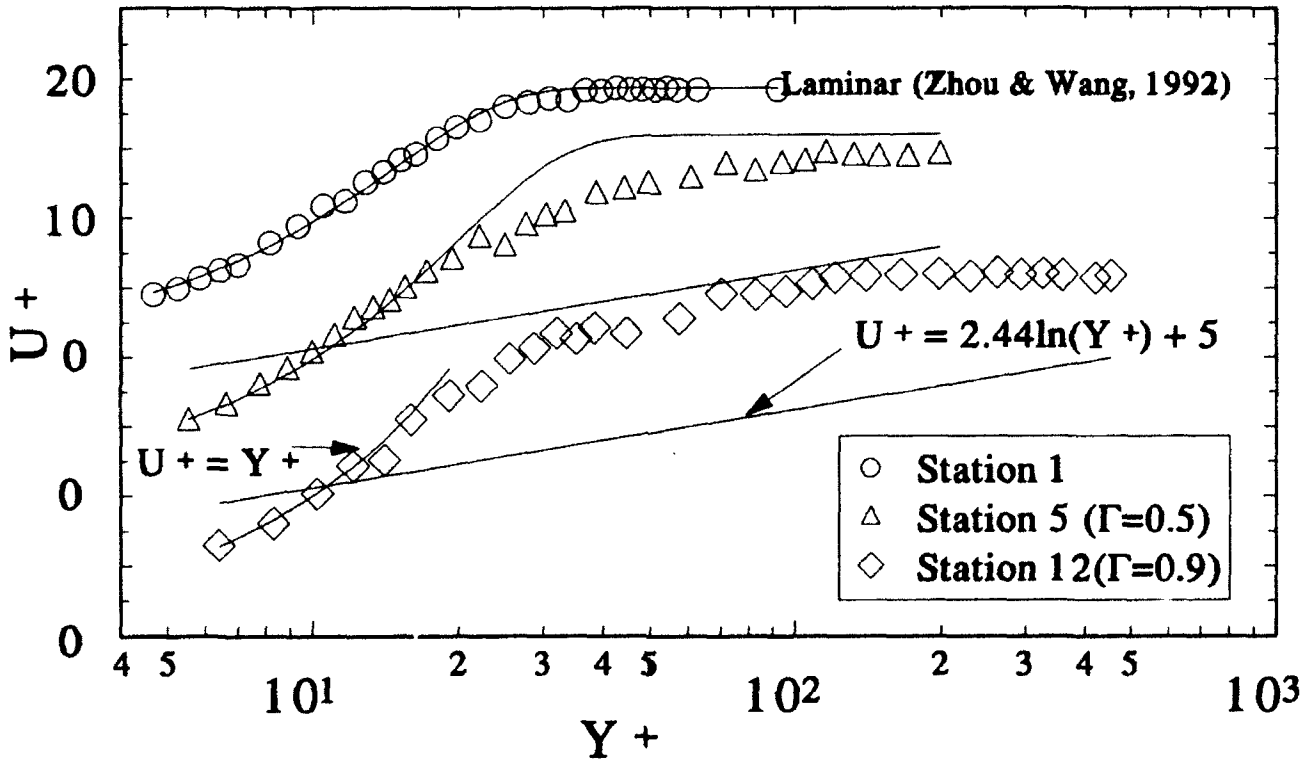

Fig. 29 Mean Velocity Profiles for G3K3 case

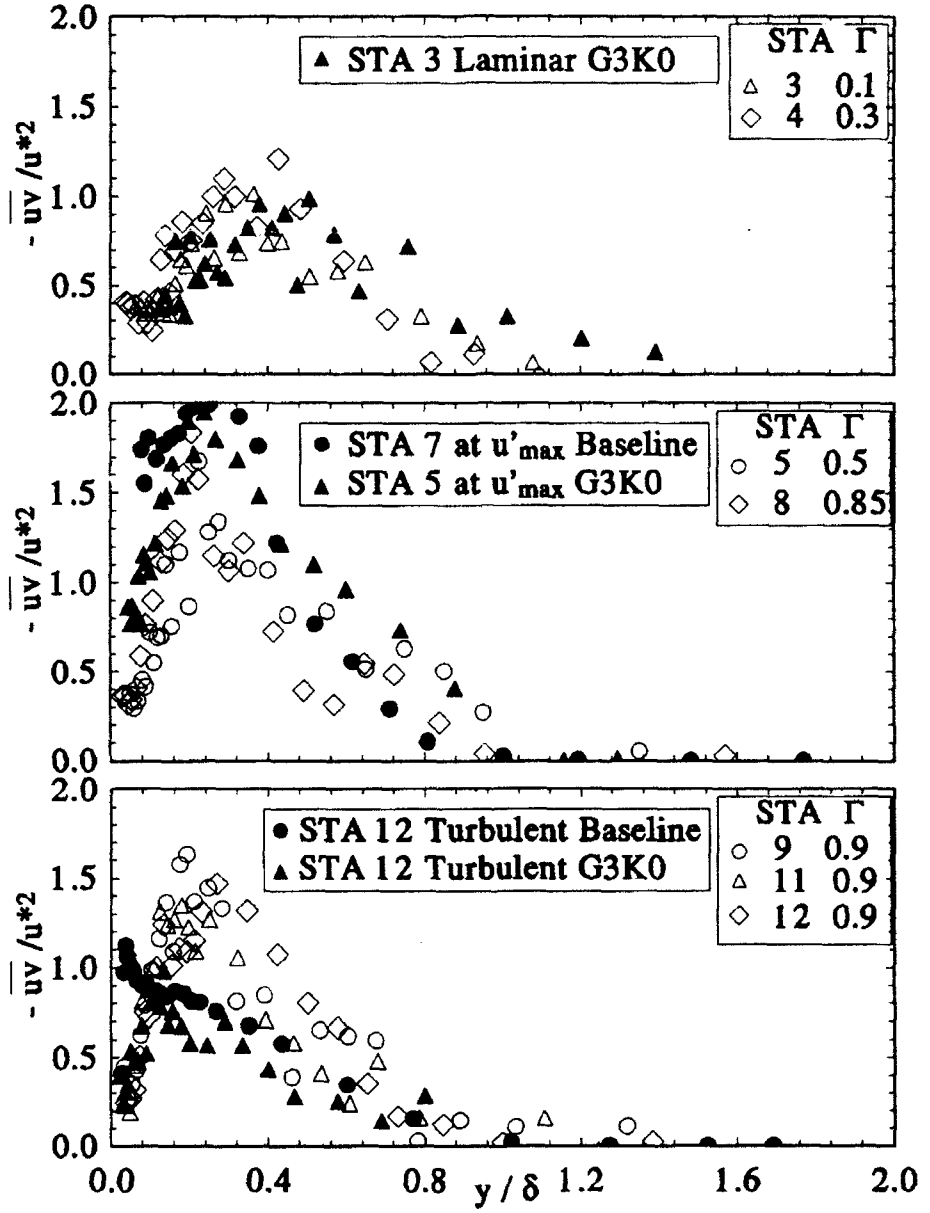

Fig. 30 Reynolds Shear Stress Distribution for G3K3 Case

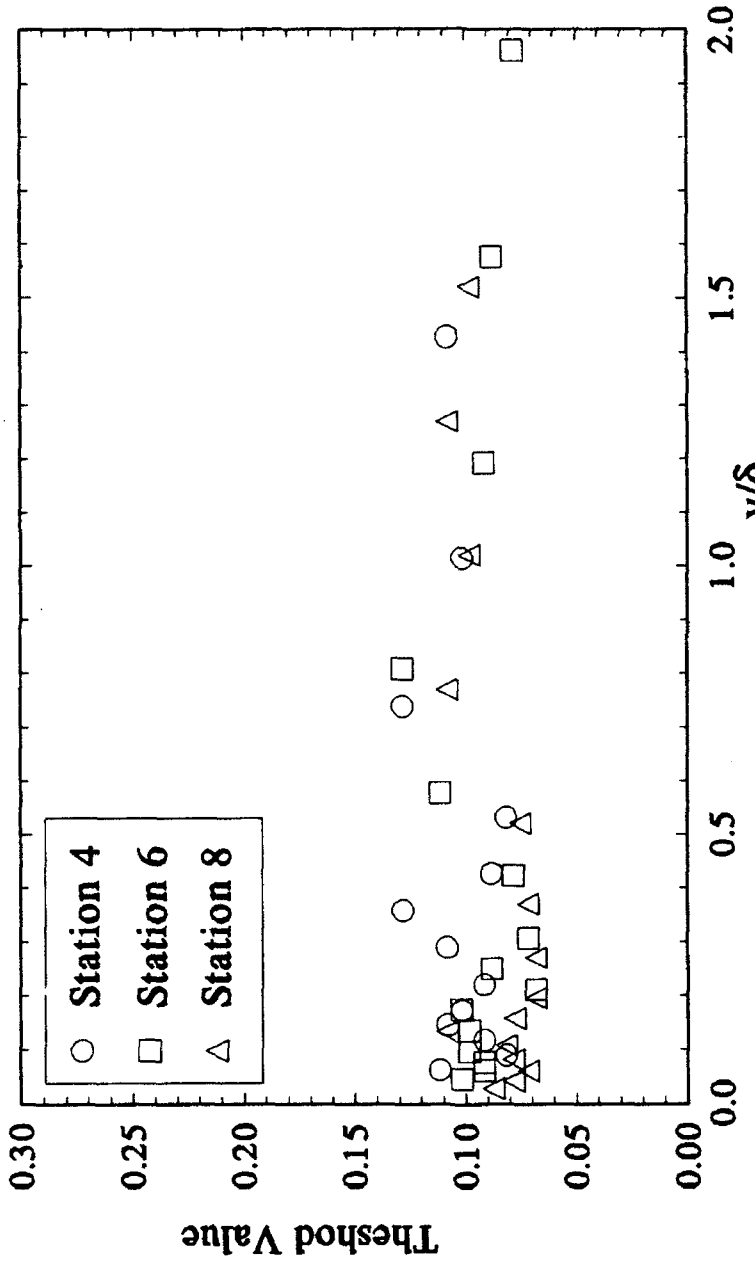

Fig. 31 Threshod Values of $(duv/d\tau)^2$

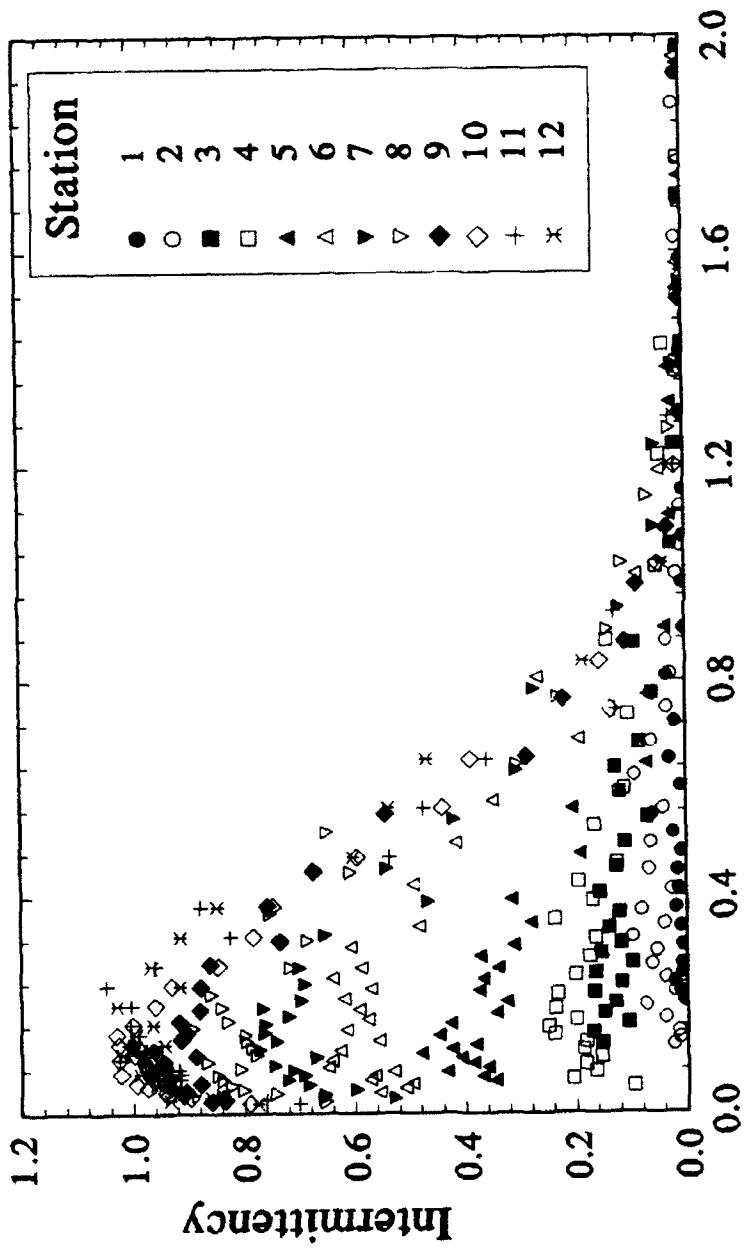

Fig. 32a Intermittency Distributions, G1 K0 Case

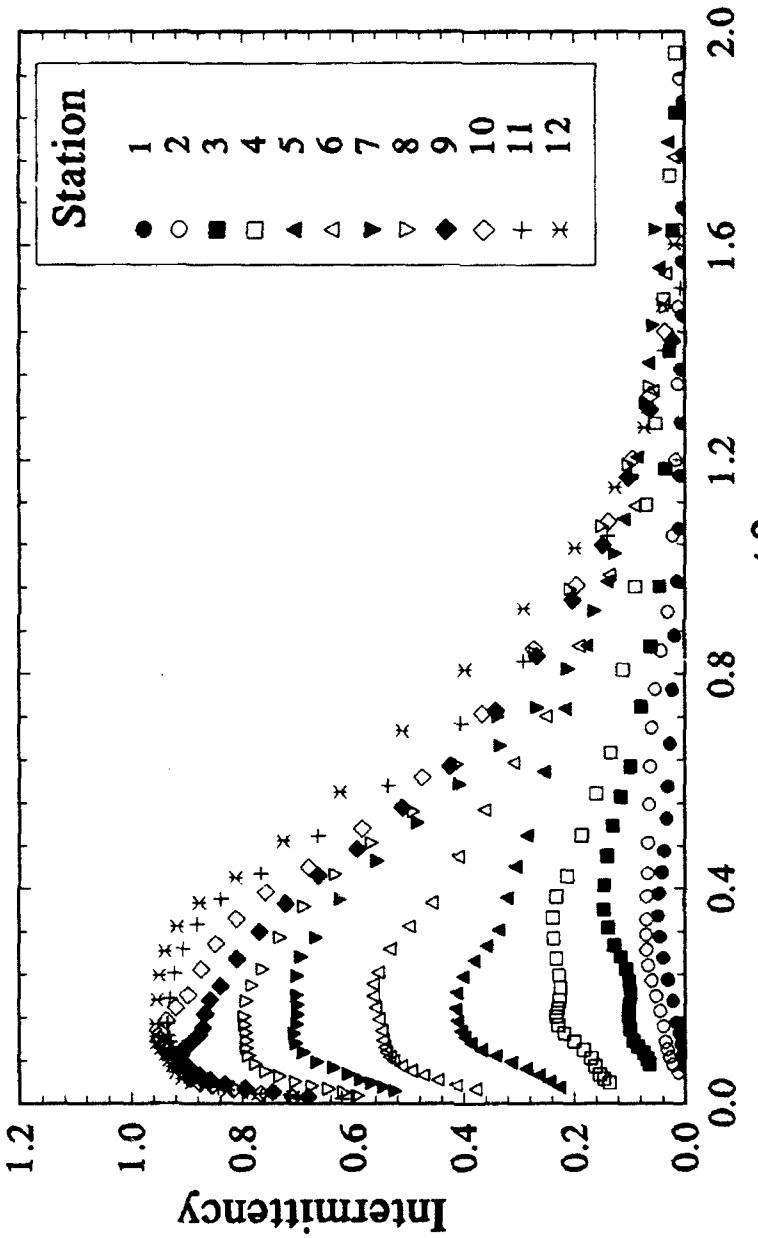

Fig. 32b Intermittency Distributions, G1K1 Case

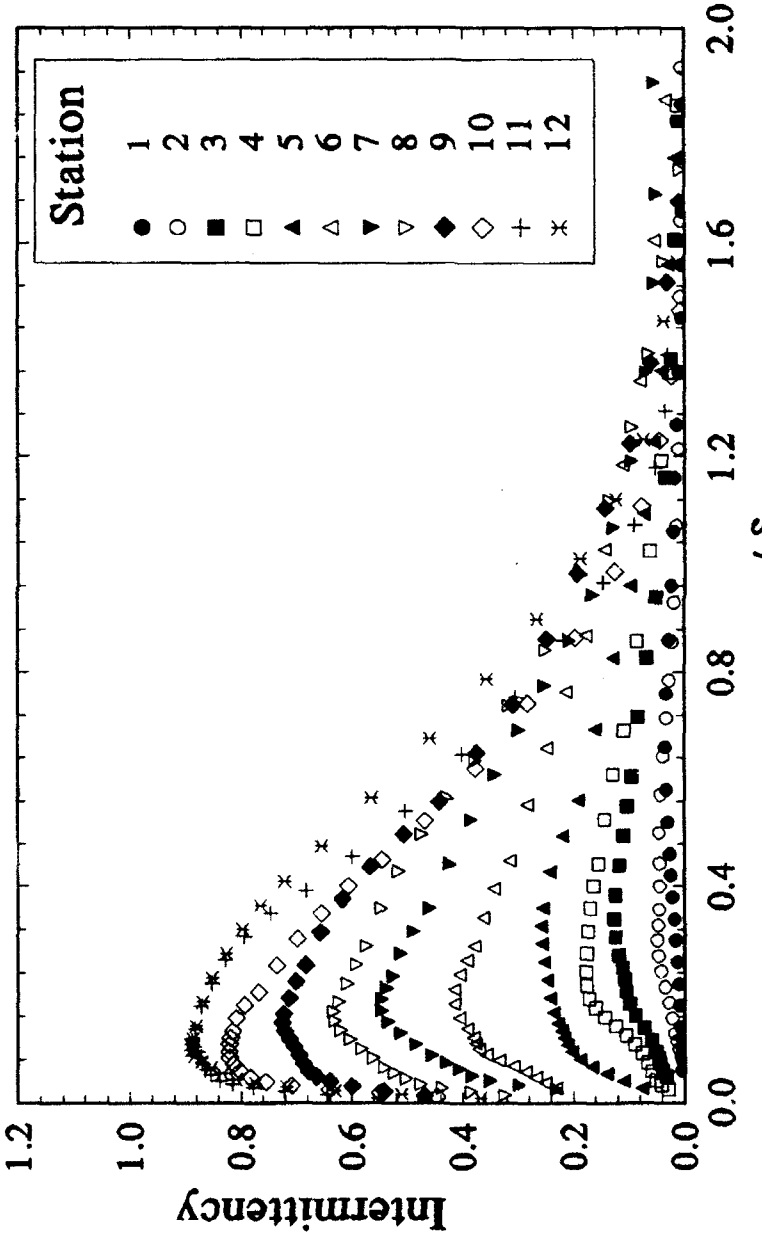

Fig. 32c Intermittency Distributions, G1K2 Case

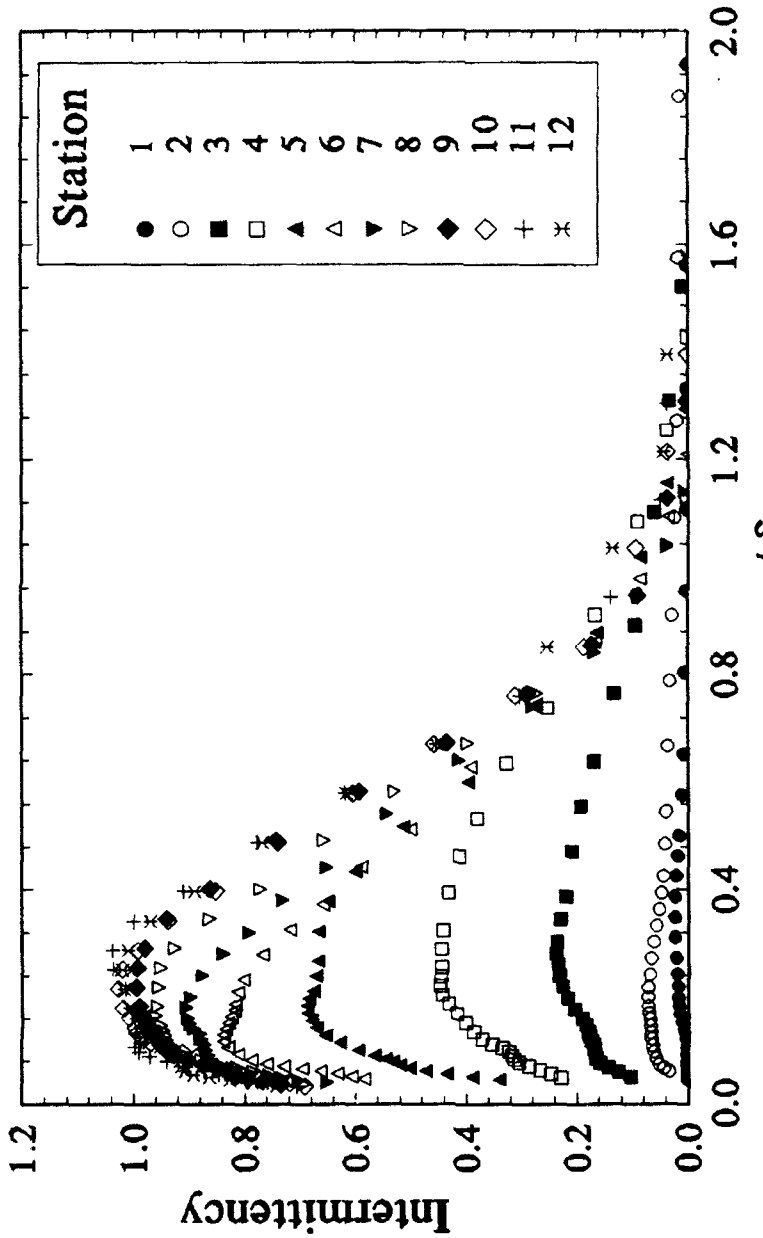

Fig. 32d Intermittency Distributions, G2K0 Case

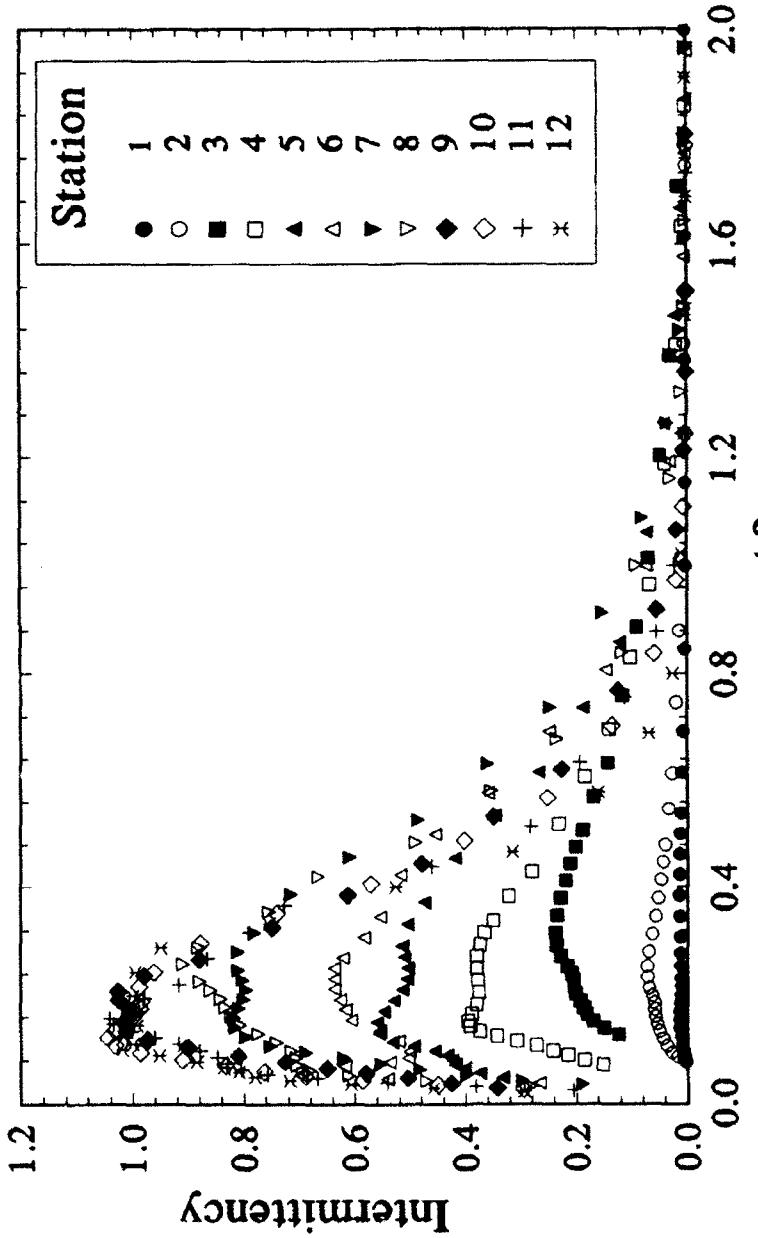

Fig. 32e Intermittency Distributions, G3K0 Case

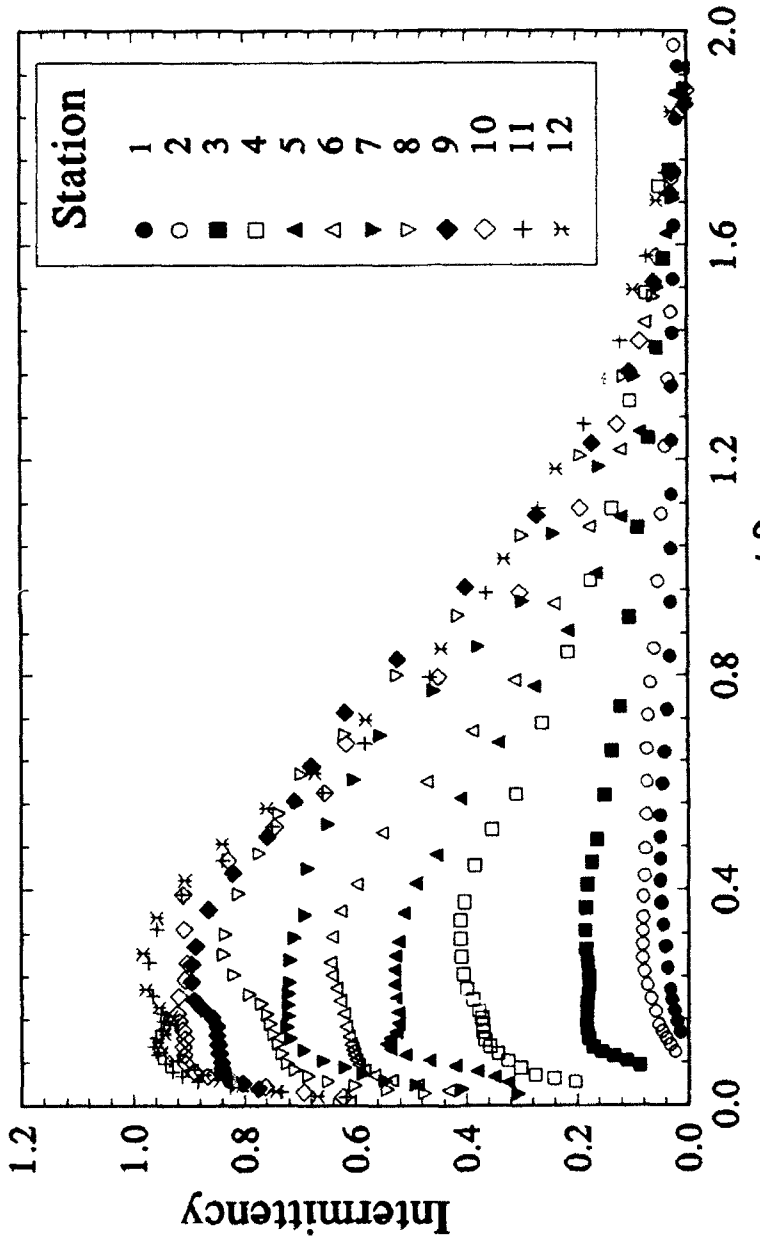

Fig. 32f Intermittency Distributions, G3K2 Case

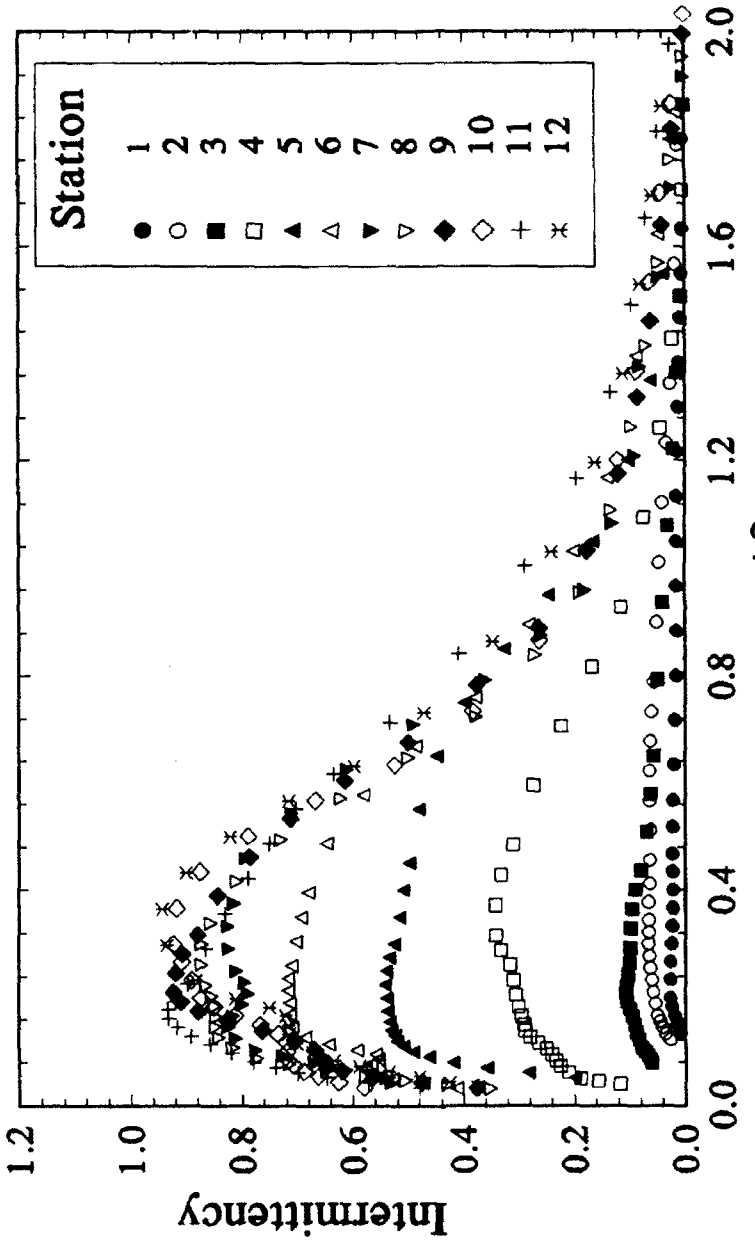

Fig. 32g Intermittency Distributions, G3K3 Case

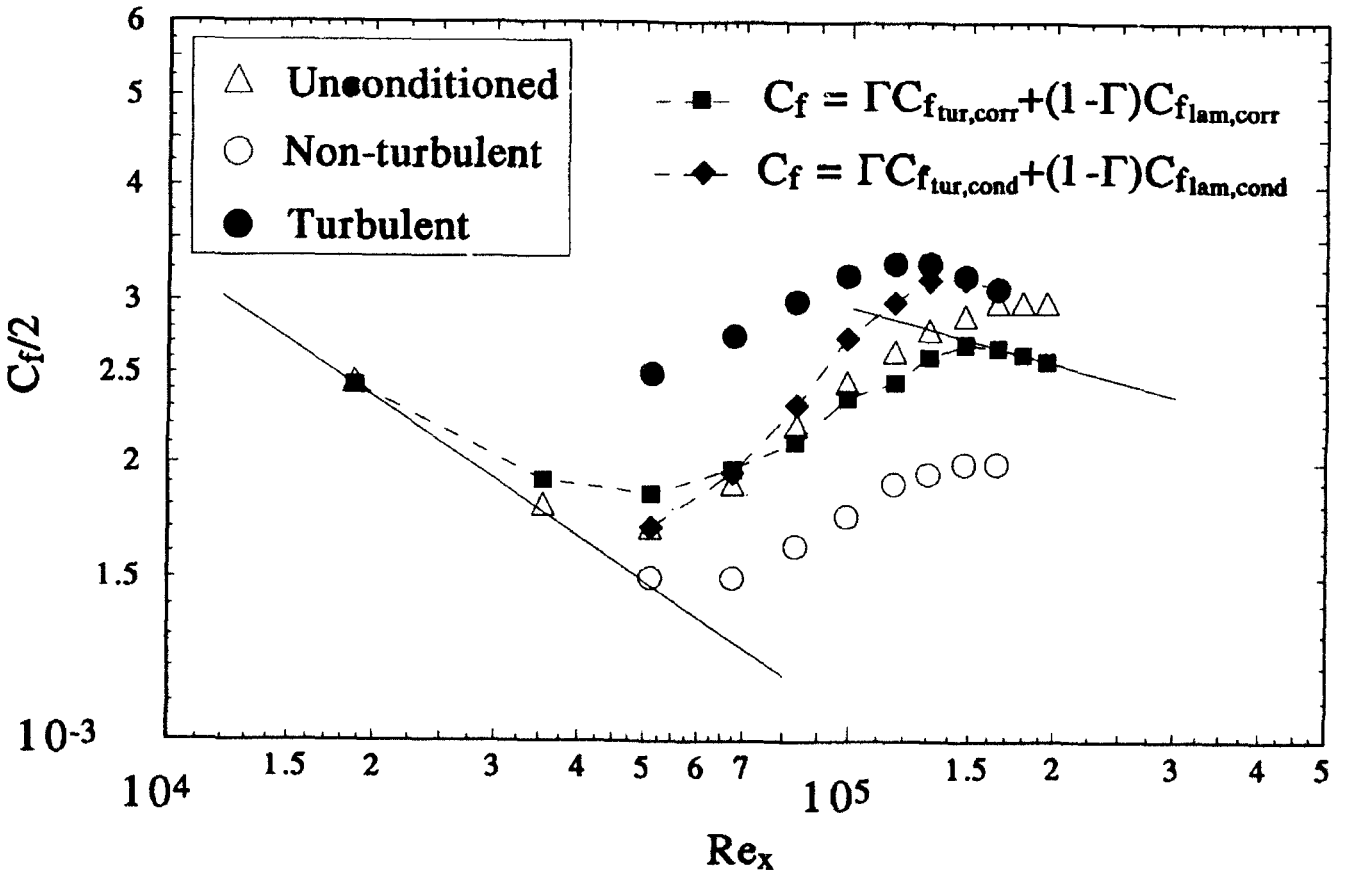

Fig. 33 Conditional Sampling Results, $C_f/2$ vs. Re_x, G3K0 Case

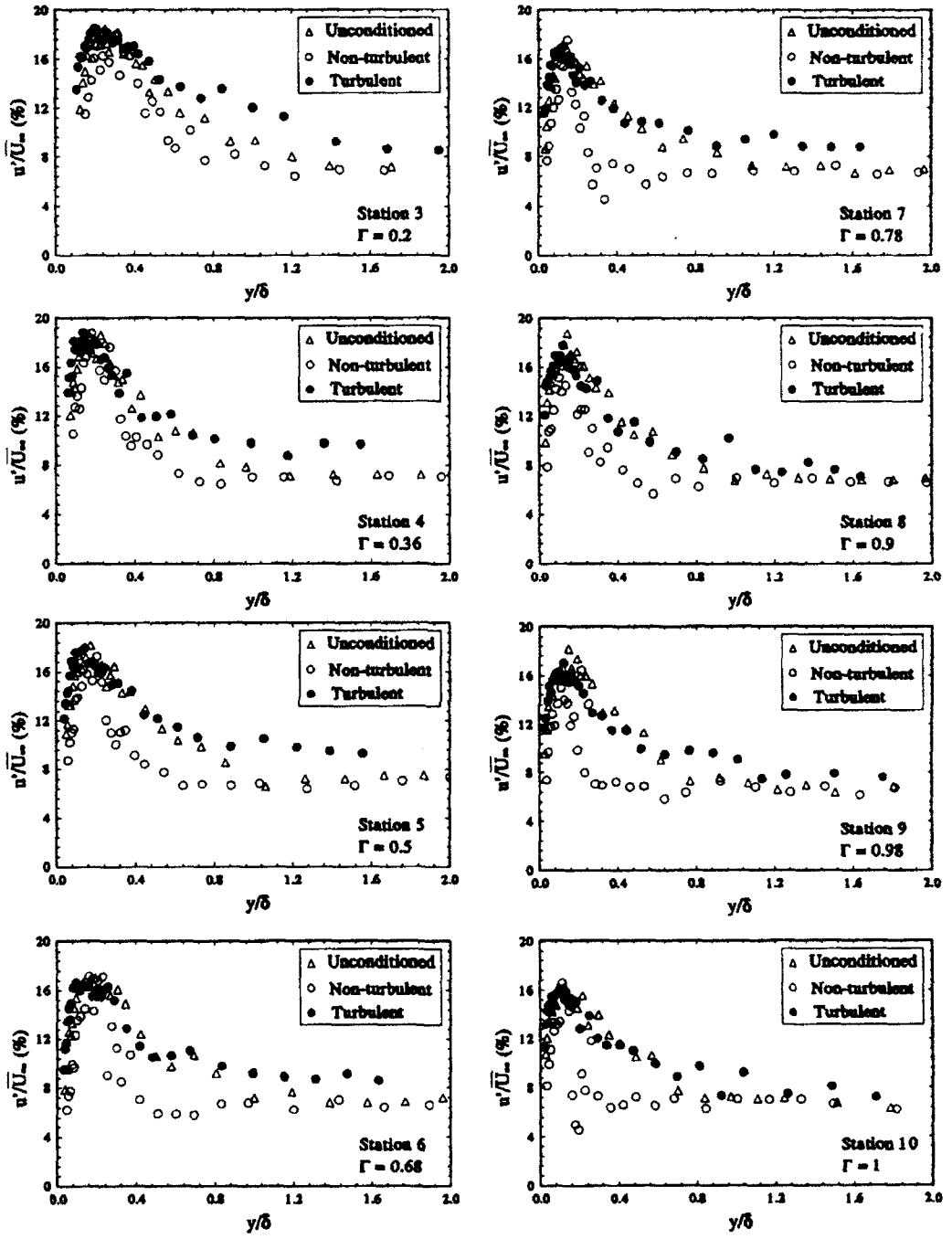

Fig. 34 Conditional Sampling Results, u'/U∞ vs. y/δ, G3K0 Case

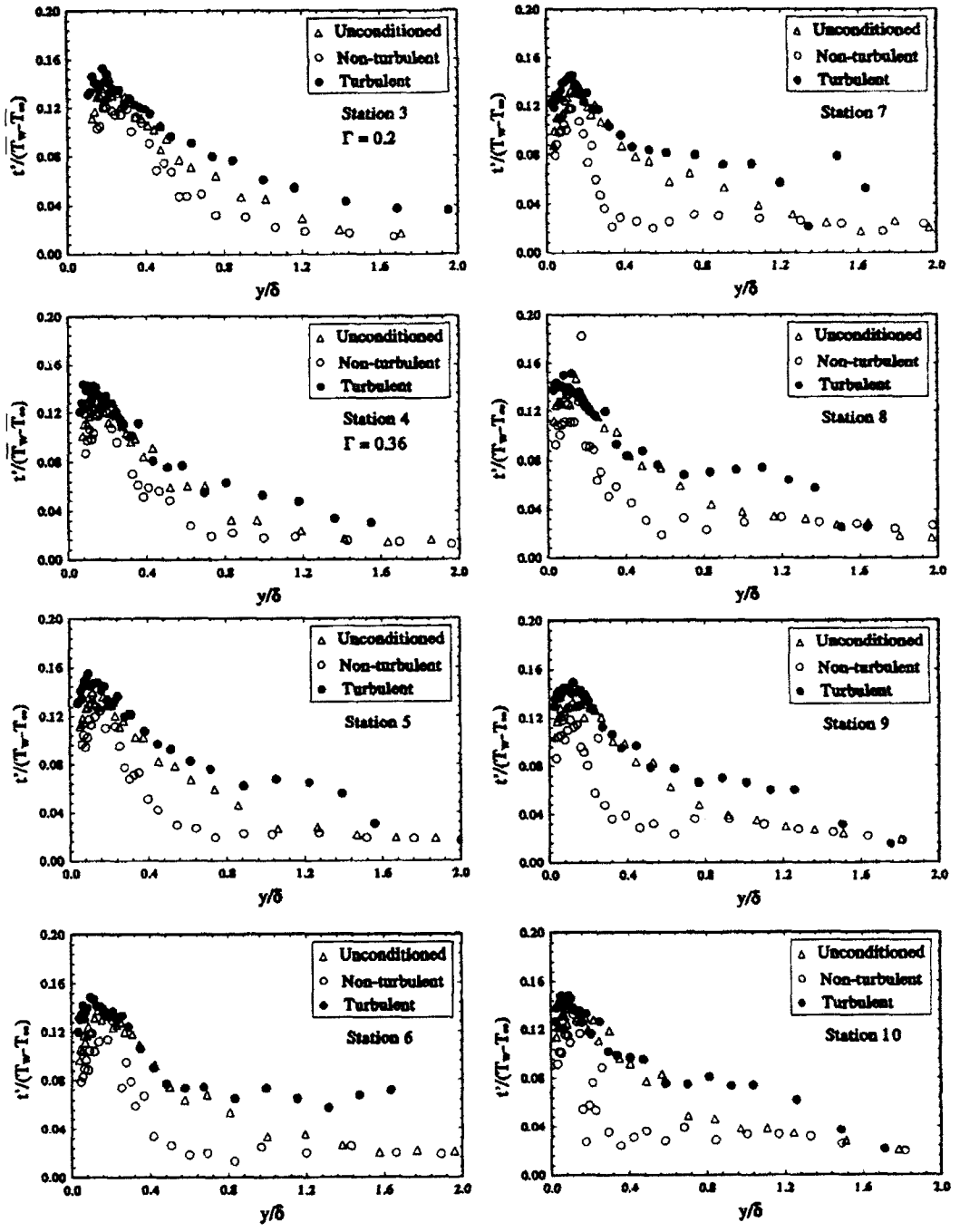

Fig. 35 Conditional Sampling Results, $t'/(T_w-T_\infty)$ vs. y/δ
G3K0 Case

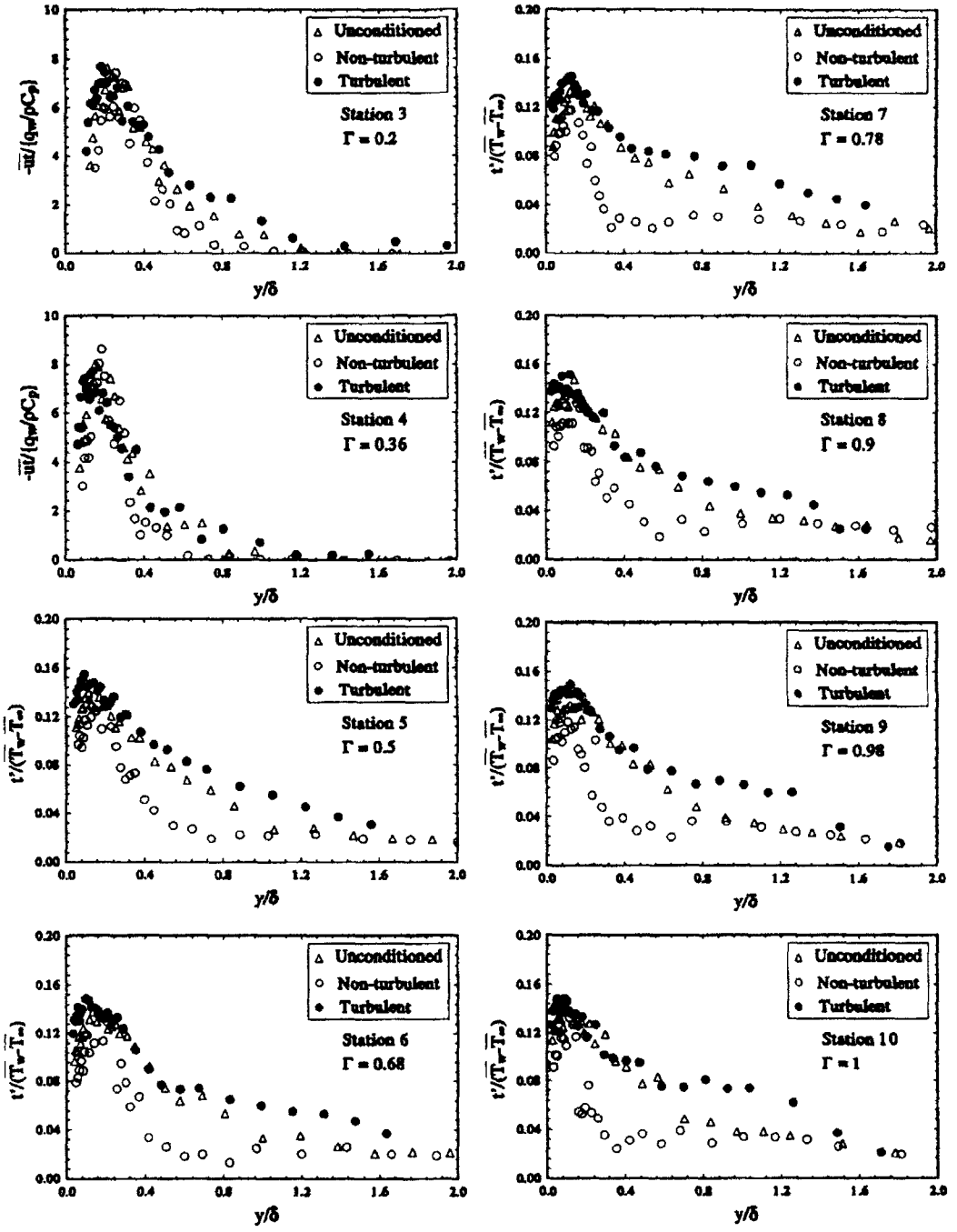

Fig. 36 Conditional Sampling Results, $-ut/\{q_w/\rho C_p\}$, G3K0 Case

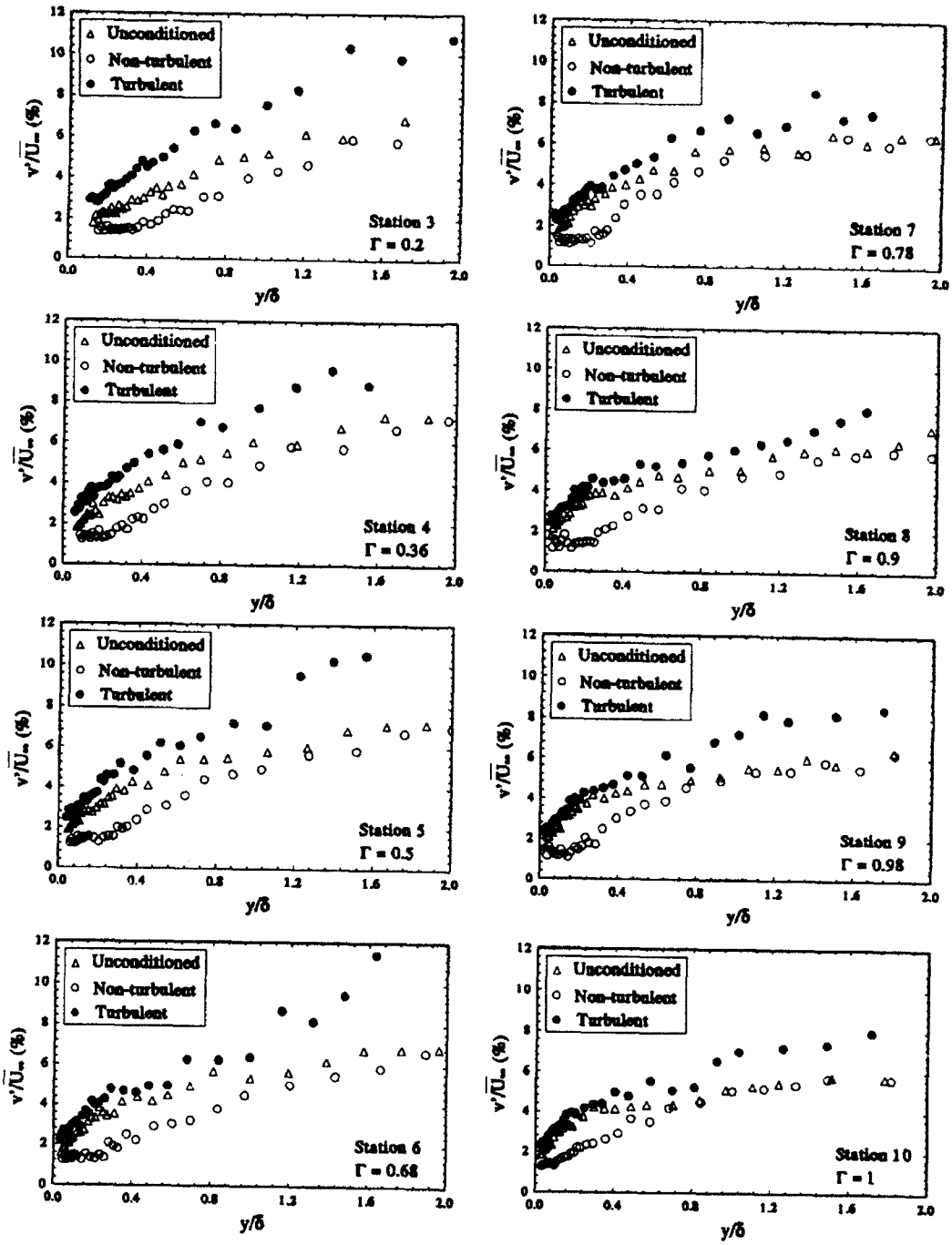

Fig. 37 Conditional Sampling Results, v'/U_∞ vs. y/δ, G3K0 Case